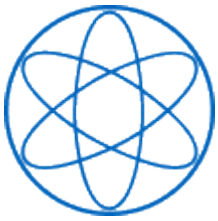

LEHRSTUHL E12 FÜR EXPERIMENTALPHYSIK

Calibration of a Light Source for single Photons in the Vacuum Ultraviolet

Bachelor Thesis

Christoph Mayr

14.08.2012

Technische Universität München

Erstgutachter (Themensteller): Prof. W. Henning

Zweitgutachter: Prof. P. Böni

Wissenschaftlicher Betreuer: Dr. J. Friese

Abstract

At the HADES experiment the detection of Cherenkov photons is used to determine the point of origin of e^+/e^- pairs. For the detection the RICH gas detector was built 15 years ago. To check its sensitivity to single photons a new light source with a light yield of some photons per msr was developed. The photons are created by the deexcitation of quasi bound molecular states of Xenon to single atoms. The light source has an adjustable photon rate and an electrical trigger signal for the RICH readout electronic.

This thesis' aim is the calibration of this new photon source in the VUV wavelength. Therefore the calibration of a Silicon diode fabricated by NIST (USA) was transferred to a solar blind PMT. Next its quantum efficiency was determined and with this result the light yield of the Xenon photon source was observed.

Table of Content

1. Motivation

The **H**igh **A**cceptance **DiE**lectron **S**pectrometer HADES at the "GSI Helmholtzzentrum für Schwerionenforschung GmbH" in Darmstadt (Germany) is an experiment dedicated to measure and study the properties of hadrons embedded in a strongly interacting medium at high temperatures and pressures. For this purpose pions, protons, and heavy ions are accelerated by the "Schwerionensynchrotron SIS18" to beam energies $E \sim 1 - 2\ A \cdot GeV$ and directed to nuclear targets located in the center of the spectrometer. The experimental setup and the physics program are described in detail in reference [1].

A **Ri**ng **I**maging **Ch**erenkov counter (RICH) [2] surrounds the target region and serves as a hadron blind trigger device for e^+/e^- pairs from meson decays produced in the nuclear collisions. A schematic view of the detector is depicted in Figure 1. Electrons and positrons from the reaction radiate Cherenkov photons when passing through the C_4F_{10} filled gas volume ($P = 1050\ hPa$) since their velocities exceed the speed of light in this medium. The photons are reflected by a spherical mirror onto the cathode pad plane of a MWPC (**M**ulti **W**ire **P**roportional **C**hamber) type gaseous photodetector and form rings of typically 4-5 cm diameter. Individual photo electrons emitted from a thin layer of CsI deposited on the MWPC cathode pads generate avalanches close to the MWPC anode wires and the respective ion cloud induced signals are registered with low noise electronic amplifier chains. On average, $N_{Ph} \sim 8 - 12$ photo electron signals are detected per ring, depending on the azimuthal and polar angle of the primary e^+/e^- - track.

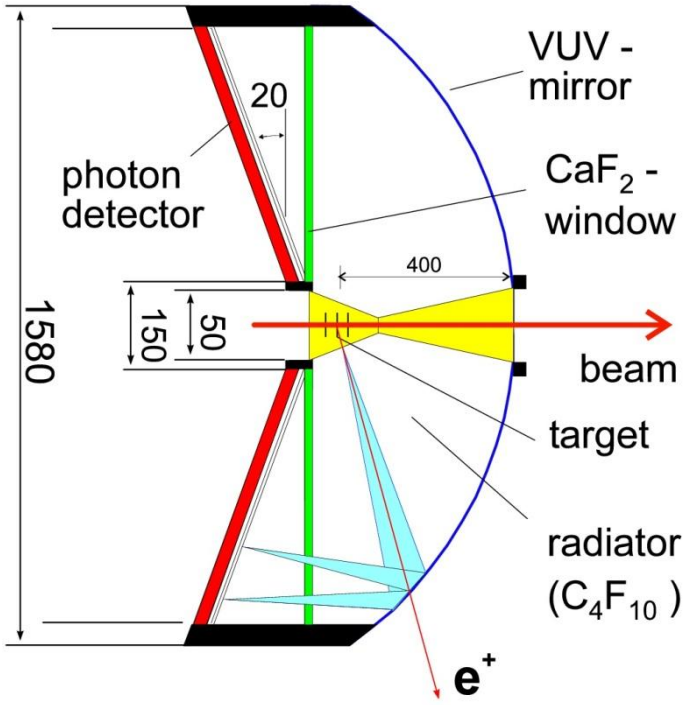

Figure 1: Cross-section of the RICH at the GSI detector with a C_4F_{10} filled radiator to emit Cherenkov light and a CsI cathode to detect it [1]

The low number of detected photo electrons is due to the short radiation length and to constraints given by the optical and electrical properties of the RICH detector components. The main constraint is given by the work function of the CsI photocathode ($W = 5.6\,eV -> \lambda_{max} = 220\,nm$) which limits the spectral sensitivity of the device to the vacuum ultra violet (VUV) wavelength region. Hence, the mirror reflectivity and the transmissions of gases and the CaF_2 entrance window play an important role. They are optimized by the usage of ultrapure materials and lead to a short wavelength limit λ_{min}~$150\,nm$. A summary plot of these optical parameters measured for small samples is given in Figure 2.

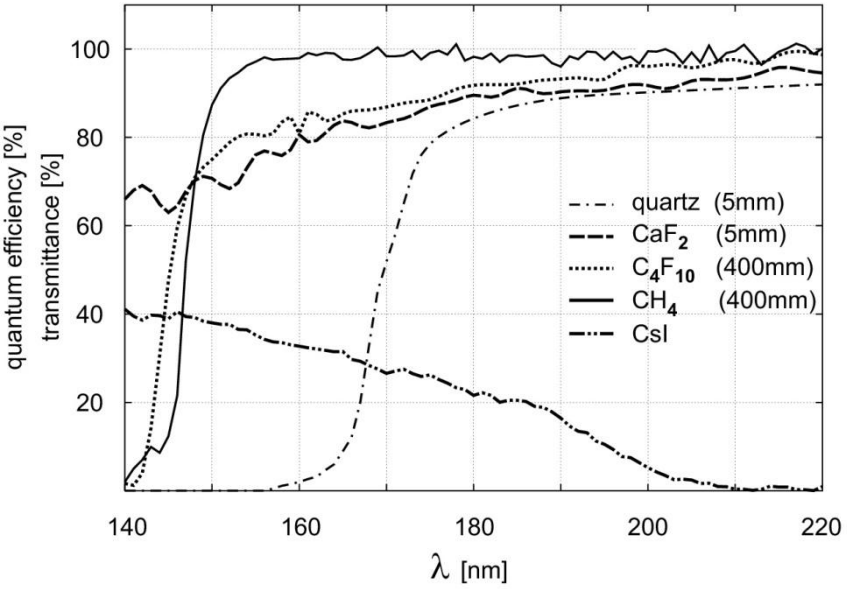

Figure 2: Transmission and quantum efficiency of the main parts of the RICH detector for wavelengths in the VUV [1]

The signal quality registered in the RICH front end electronics is governed by the gas gain achieved in the avalanche amplification of the MWPC (typ. $3 - 5 \cdot 10^4$) and the electronic noise level. Under standard experimental conditions, single photo electron detection efficiencies $\epsilon_{s.e.} \sim 90\% - 95\%$ have been achieved.

The total detection efficiency ϵ_{RICH} for primary e^+/e^- tracks is strictly governed by the ring recognition efficiency which in turn depends on all the above mentioned parameters. Up to now and due to the lack of a suitable Cherenkov light source, ϵ_{RICH} was determined from a sophisticated combination of data analysis of heavy ion reactions and detector simulations. The detector parameters were taken from measurements performed during the construction phase. Meanwhile, the RICH detector is in operation since 1998, with the transmission of the detector gases controlled and monitored over the whole period. It is well known that on the long range all gaseous detectors suffer from ageing effects which deteriorate the quality of the signals to be detected. A remeasurement of the Cherenkov light detection efficiency in the RICH has thus become mandatory.

Recently, the RICH group has started this remeasurement project and developed a new light source [3] operated in pulsed mode with appropriate emission and intensity characteristics. The source provides a fast trigger signal needed for the readout of the RICH photon detector and rather low photon intensity per pulse to allow single photon detection. The new source is designed to perform

efficiency measurements of the integrated system without requesting ion beams from the accelerator facility and full spectrometer operation. Within this project, the intensity calibration of the new light source is of crucial importance. However, for such weak light sources in the VUV region absolute light yield calibration has turned out to be notoriously difficult and unreliable.

The present bachelor thesis is an attempt to address this difficult task. The thesis is organized as follows. After a more detailed description of the new single VUV photon source the chosen calibration procedure is discussed and the experimental set-up described. In the following chapters, systematic measurements with a solar blind photo multiplier tube are reported. Finally, a quantitative evaluation of the VUV light emission of the new source is presented.

2. The new VUV photon source

2.1 General requirements

The in-situ measurement of the HADES RICH photon detector response to single photons requires a light source with emissivity in the VUV spectral region $150\ nm < \lambda < 200\ nm$. The source needs to be located in the optical center of the RICH (see Figure 1) replacing the target and beam tube area. Preferentially it should illuminate the whole forward hemisphere (i.e. $\sim 2\pi$ solid angle). The detector geometry and the cathode segmentation into ~ 28000 pixels requires a moderate light yield of less than $5 \cdot 10^4$ photons per pulse, when aiming at an areal photon density $\rho < 1\ photon/pad$ on the photo cathode plane. In addition, each light pulse should be accompanied by a fast electronic trigger signal which starts the electronic readout only at the time of photon appearance at the pad plane. Otherwise, the single photon signals would be indistinguishable from randomly coincident noise signals in the detector. The realized solution is a bulb of fused silica filled with high purity Xenon gas. The light emission is excited by means of alpha particles from a radioactive ^{241}Am source.

2.2 Excimer emission of Xenon gas

The ideal candidates for a quasi-continuum light emission in the $150\ nm < \lambda < 200\ nm$ region are Xenon gas molecules formed in so-called excimer (excited dimer) states. After a Xenonatom is excited it may undergo collisions with other atoms and form excimer molecules with lifetimes of a few nanoseconds. This process is described in more detail in ref [4] and involves the energetic level scheme as shown in Figure 3 (left panel). Deexcitation of the quasi bound molecular states $6s[3/2]_1$ or $6s[3/2]_2$ to the repulsive ground state of 2 close by atoms yields photons with a broad spectral distribution and a peak wavelength $\lambda_{peak} = 174\ nm$ (see right panel of Figure 3). The efficiency of the molecular formation process and hence the light output is strongly related to the presence of gas admixtures. This requires the usage of highly purified Xenon gas in the newly constructed light source.

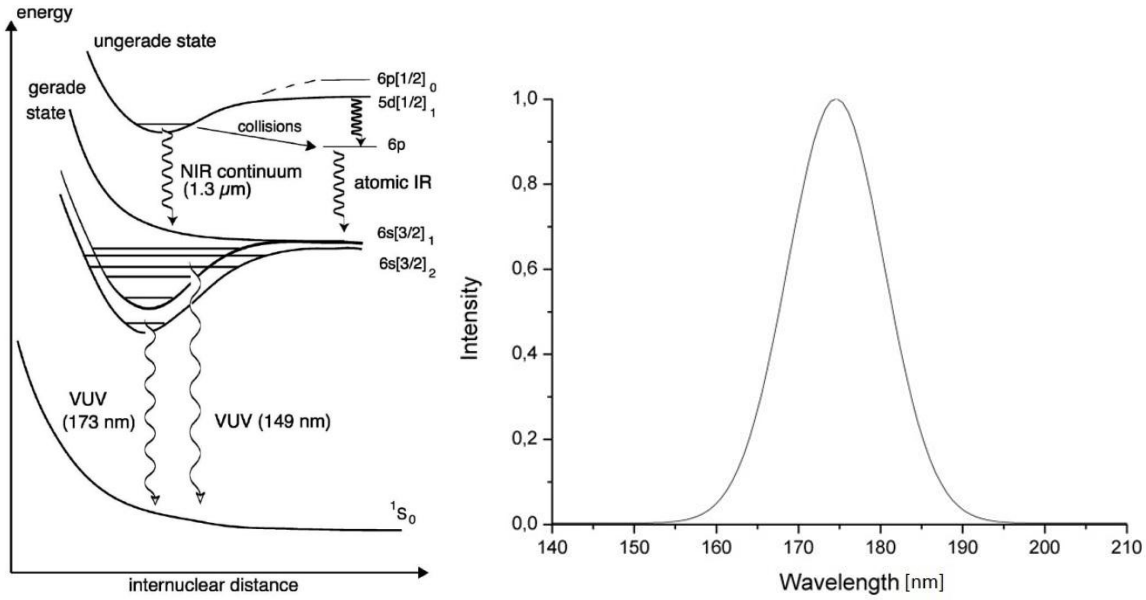

Figure 3: left: Energy states of Xenon gas with possible transmissions from excimer molecules to unbound atoms [5]
right: VUV spectrum of photons emitted by the deexcitation of Xenon excimer molecules [4]

2.3 Photon yield of alpha induced excimer emission

One possible way to excite the Xenon gas atoms is to use the energy loss released by energetic charged particles in the gas. The particle species range from electrons ($\sim 100\ keV$) up to heavy ions ($5 - 100\ A \cdot MeV$) [7]. Helium ions (alpha particles) of a few MeV deposit their energy in a well confined gas volume and are easily available from radioactive sources. The light output obtained for alpha induced excimer excitation in noble gases at various pressures has been measured [4] and is shown in Figure 4. The light output for Xenon is perfectly matched to the needs of the new VUV light source. With alpha particles from an ^{241}Am source ($E_\alpha = 5.48\ MeV$) fully stopped in Xenongas at a pressure $P = 1200\ hPa$ a light yield (in 4π) of $N_{ph} = 1.6 \cdot 10^5$ photons/alpha is expected.

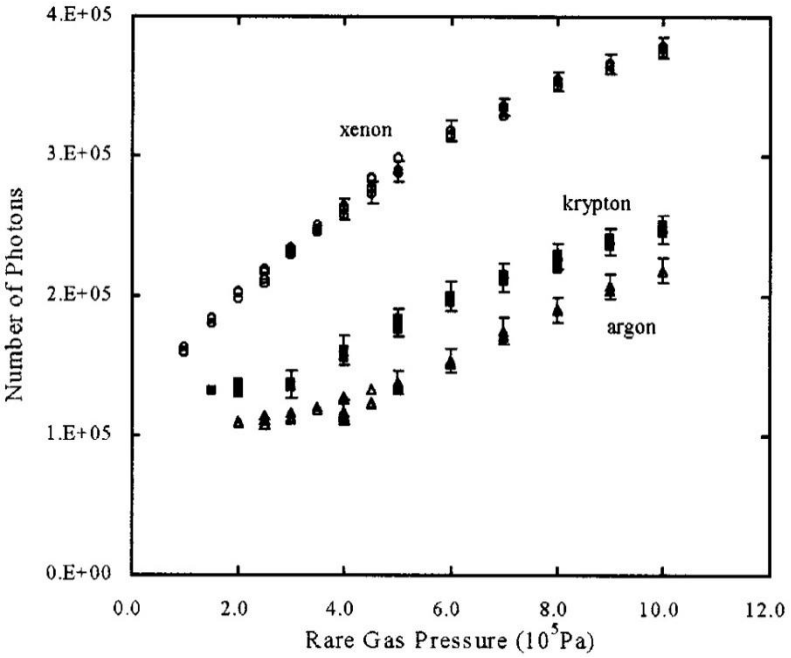

Figure 4: Variation of the number of scintillation photons in noble gases excited by 5.49-MeV alpha particles in the pressure range from $\mathbf{1.0 \cdot 10^5}$ Pa to $\mathbf{10.0 \cdot 10^5}$ Pa. [4]

2.4 Layout of the Xenon VUV source

The alpha particles used for the Xenon excitation offer the possibility to generate a fast trigger signal. If not fully stopped in the gas, they can be detected by means of a silicon detector like a PIN diode. For energy depositions above $200\ keV$ in the PIN diode, standard electronic amplifiers deliver fast signals with a timing resolution $\tau < \sim 10\ ns$. For ^{241}Am activities around $A \sim 10\ kBq$ this is sufficient to identify individual alpha particle triggers even at very close distances between detector and source.

The resulting layout of the new VUV photon source is depicted in Figure 5. A stainless steel tube mounted on a flange with feed throughs for gas, signal and power supply cables is designed such as to fit exactly into the beam tube hole of the RICH photon detector. The front part is connected to a cylindrical bulb (quartz glass tube) made of fused silica [6] which houses a custom designed, point like ^{241}Am source ($A = 10\ kBq$) located opposite to a silicon PIN diode ($F = 100\ mm^2$). The volume is gas tight and filled with Xenon gas (Purity 5.9) to a pressure $P_{Xe} = 1200\ hPa$.

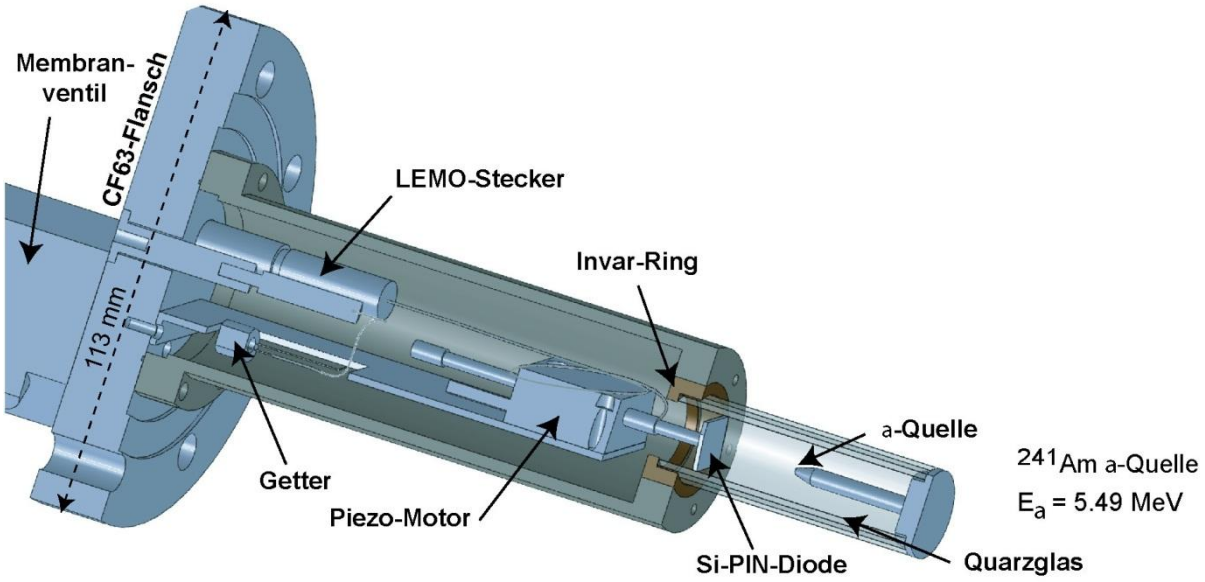

Figure 5: Schematic cross-section of the Xenon filled VUV photon source with an ^{241}Am alpha source and a moveable PIN-Diode [5]

The transmission curve of fused silica (Figure 6) fits well to the excimer emission range, although losses for short wavelengths $\lambda < 170\ nm$ are expected. At the given pressure the range of the $5.484\ MeV$ alpha particles is $R{\sim}18 - 20\ mm$. The distance between PIN diode and alpha source ($1\ mm < D < 20\ mm$) can be adjusted by means of a piezoelectric linear drive. In this way the trigger rate as well as the light output per alpha particle can be varied significantly. Typical trigger rates range from $\sim 4\ kHz$ down to $100\ Hz$, allowing for excellent statistics of single photon hits on the RICH detector plane within reasonable measurement time. For fresh and pure gas and taking the transmission of fused silica into account, a maximum light yield of $N_{ph} \sim 1.2 \cdot 10^5$ photons/alpha is expected (at $D = 20\ mm$). However, any gas impurities from outgassing of inner surfaces may significantly reduce this number.

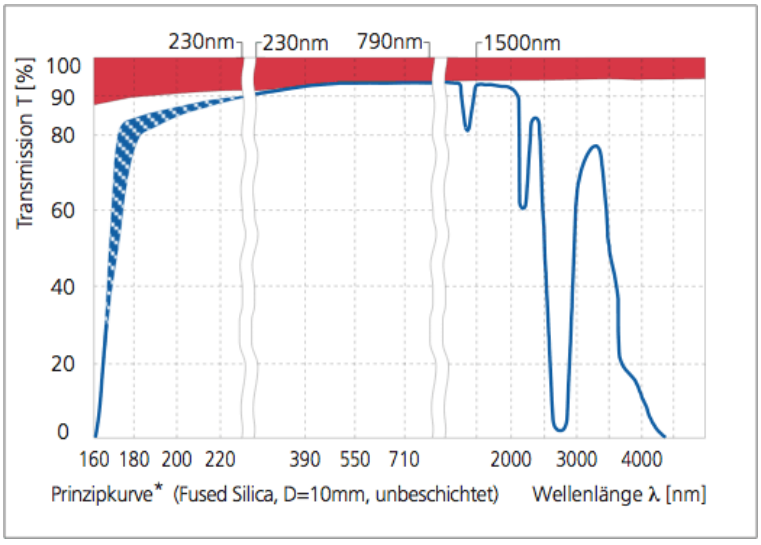

Figure 6: Transmission of fuesed silica for wavelengths between 150 and $5000\ nm$

3. The Calibration Setup

3.1 General considerations

The aim is to determine the number of photons per trigger signal of the VUV photon source. Therefor a gauged photo detector is needed. A silicon diode that is also sensitive for wavelengths in the VUV range is a good choice and is available in the institute. [7]

The emission of the photon source cannot be measured directly with the Si-diode, because the electronic noise of the photo diode is larger than the signals of single photons. Therefore it is necessary to do an intermediate step, i.e. to calibrate a detector that is able to detect single photons. This detector has to achieve the following properties:

- Quantum efficiency in the VUV range as the detector is finally used to calibrate the VUV photon source
- Low noise so single photons can be detected
- High gain in order to have a measurable output signal for single photons

Therefore a solar-blind photomultiplier tube is the perfect match and if the PMT is calibrated it should be possible to assign this calibration to the VUV photon source.

For the calibration of the PMT with the help of the Si-diode it was provided a reasonably intense and stable VUV light source. Apertures were used to reduce the photon flux in order to run the PMT in the 'counting mode'. In this mode the signals of incoming single photons are counted. To achieve a low number of photons several possibilities are suitable, like:

- Measuring at air pressure so that the O_2 and H_2O molecules absorb a certain amount of photons
- Using a filter or aperture to reduce the lamp's light
- Using a wavelength where the PMT has a small quantum efficiency
- Increasing the distance between the lamp and the PMT
- Using smaller apertures in front of the PMT

The first two options would also reduce the light at the Si-diode which leads to small photo currents and thus bigger uncertainties connected to the measurement of the current. The other three possibilities could be applied. Hence, a setup with variable path lengths, apertures and wavelength filters has been set up and will be described as follows.

3.2 Experimental details

3.2.1 Overview of the setup

A schematic view of the main parts of the calibration set-up can be seen in Figure 7. The set-up was already used in another experiment and only few adaptions were necessary.

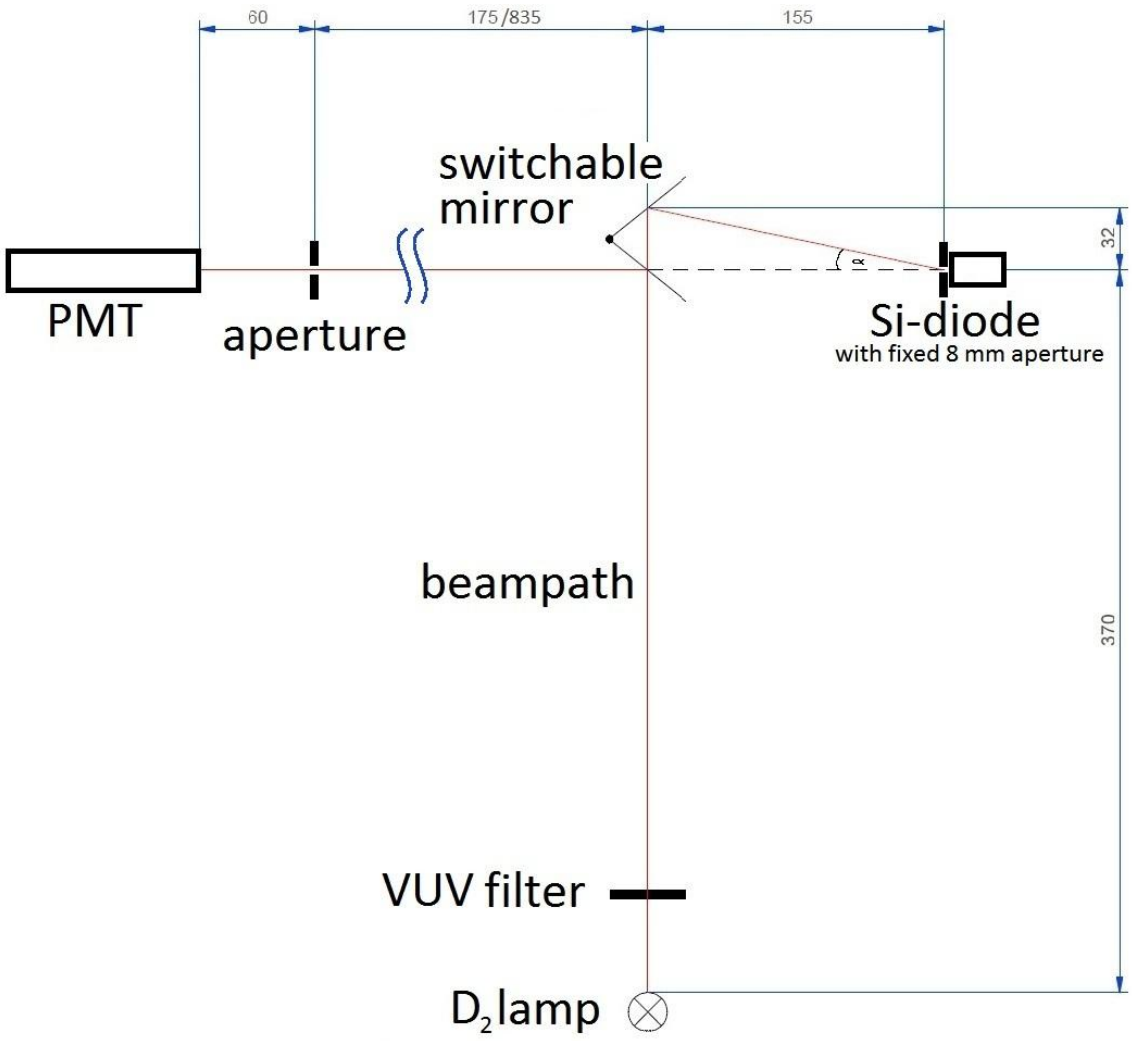

Figure 7: Schematic set-up to calibrate the PMT. The lengts are stated in mm and can bee seen in Table 1.

As the measurements were made with VUV light the set-up was in an evacuable steel cylinder. On the bottom of the schematic drawing a Deuterium arc lamp can be seen which provides a continuous spectrum in the VUV range (see chapter 3.2.2). Furthermore the lamp emits enough light so the Si-detector can work. The device between the lamp and the steel cylinder is used to mount different wavelength filters without breaking the vacuum (see Figure 8). Furthermore there is a mirror in the

cylinder to switch the beam between the Si-diode (on the right) and the PMT (on the left). This enables a prompt measurement at the two photo detectors. The beam path has an offset of $3{,}2\ mm$ of the cylinder's center if the right detector is radiated, because the mirror's center of rotation is not exactly in the middle of the cylinder. Therefore the beam does not hit the detector on the right side vertically. The distance between the mirror and the PMT can be extended with the help of an additional steel tube with a length of $660\ mm$ to decrease the PMT's solid angle. An aperture in the pipe in front of the PMT controls and changes its solid angle. Also in front of the Si-diode there is an aperture with a fixed diameter of $8\ mm$. Figure 8 shows a photo of the set-up.

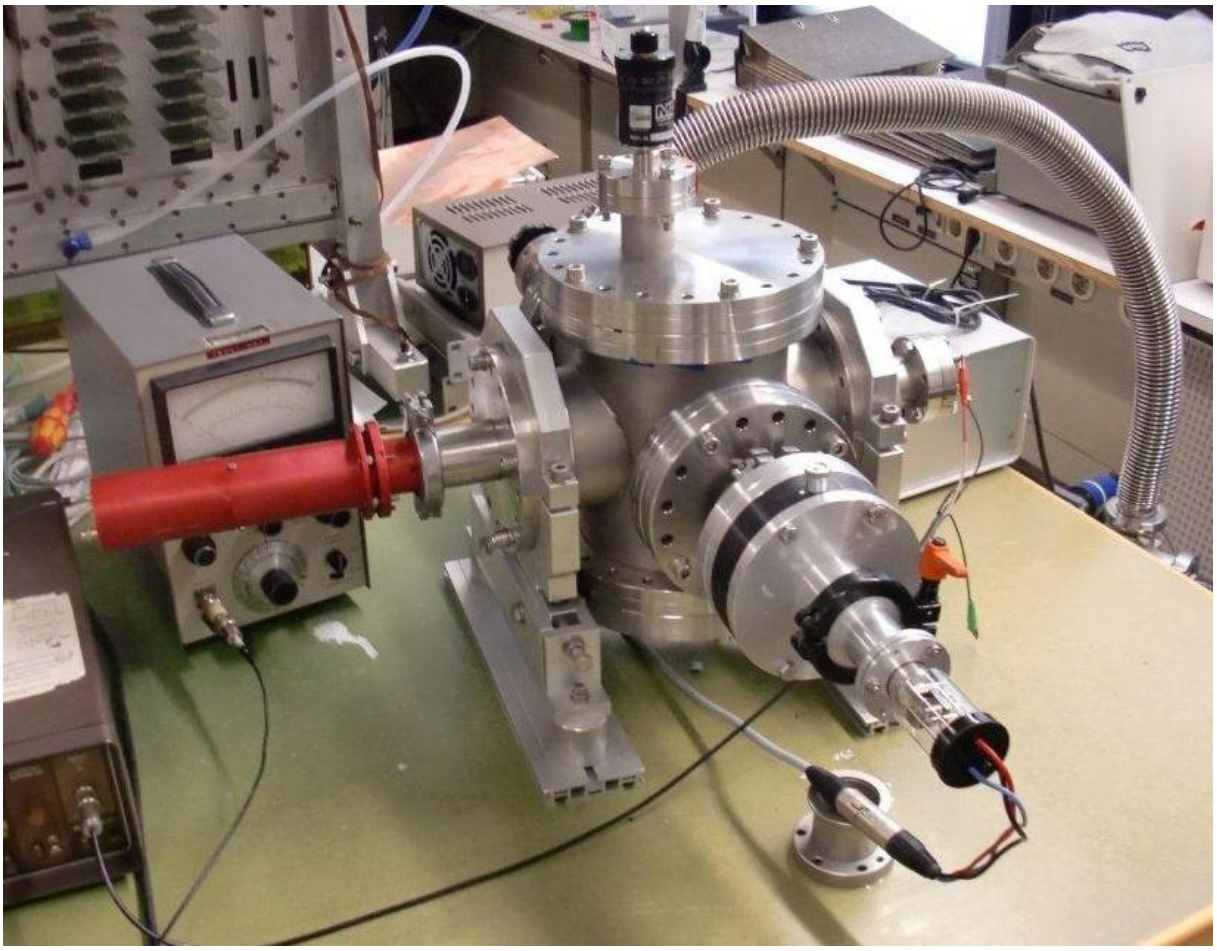

Figure 8: Picture of the stainless steel cylinder with the PMT (left flange), the Si-diode (right flange), the D_2-lamp and the gadget to change the different filters (front flange).

Two ampere meters were used to measure the currents. Because the currents were partly in the pikoampere range special current meters were needed. The PMT's current was measured with the KEITHLEY 602 and the Silicon diode's with the KEITHLEY 614. Pictures and specifications of them can be seen in the appendix #2. [8]

The lengths of the set up are listed in the following table with their uncertainties.

	Length [mm]	Uncertainties [mm]
Lamp – Mirror (right side)	402	±5.8
Mirror – Si-diode	158	±6.5
Lamp – Mirror (left side)	370	±5
Mirror – Aperture	175	±5
Mirror – Aperture (with additional pipe)	835	±5.4
Aperture - PMT	60	±4

Table 1: Distances in the set-up for calibrating the PMT

3.2.2 The Deuterium Arc Lamp

The radiation of the light source has to be strong enough so that the photocurrent of the Silicon diode is still measurable. Furthermore a part of its spectrum needs to be in the VUV range, because the PMT is only sensitive for wavelengths shorter than $200\ nm$. Finally the spectrum should be continuous in this range.

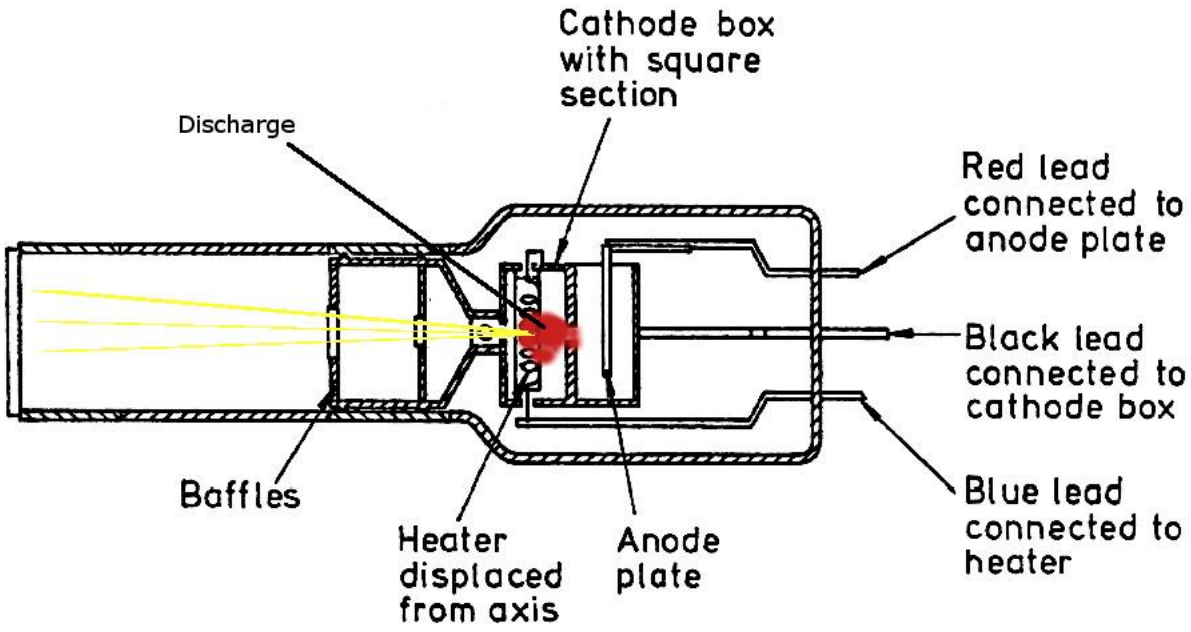

Figure 9: Schematic build-up of the Deuterium arc lamp. The light emitted in the discharge region gets focused with the help of apertures and the photons leave the lamp through a window at the left side [9]

The deuterium arc lamp matches these requirements. The housing contains a filament wire and an anode which accelerates free electrons from the filament wire towards itself. The lamp is filled with

deuterium gas and on their way to the anode the electrons excite deuterium molecules to higher energy states. The decay of these excited molecules into two atoms release photons in the VUV range. The reaction is:

$D_2 + E_e \rightarrow D_2^* \rightarrow D' + D'' + h\upsilon$ [10]

where $E_e$is the electrical energy and D_2^* is the excited Deuterium molecule. The energy of D_2^* is quantized, whereas the energy of the atoms ($D' and\ D''$) is not. Their energy is only based on their relative kinetic energy and can be continuous between $0 \leq E_{D'} + E_{D''} \leq E_{D_2^*}$. This means that the photon's energy is also continuous and has wavelengths from $160\ nm$ to visible light.

Figure 10 shows the spectrum of the deuterium arc lamp in the region between $115\ nm$ and $300\ nm$ (black line).

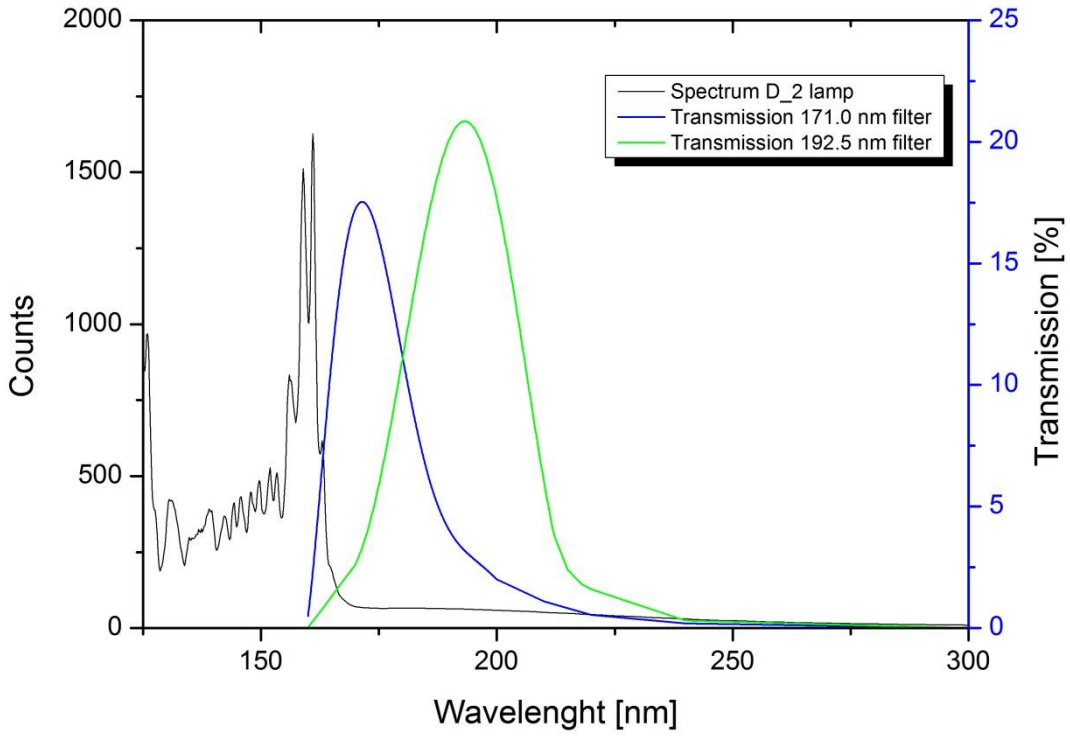

Figure 10: The Deuterium arc lamp's spectrum in the range of 130 nm to 300 nm [11]and the transmission of the used monochromators in the same area [12]

The light output of the lamp also depends on its temperature. To start the lamp the filament wire needs to be heated for several seconds. After that the discharge progress produces enough heat to shut down the heater and to hold the filament's temperature. It takes about one hour for the radiation to be stable enough to make a precise measurement.

3.2.3 The VUV filters and the apertures

The VUV filters used in this experiment are manufactured by "Pelham Research Optical LLC". They are needed, because the spectrum of the Deuterium lamp is not only in the VUV range but also in the area of visible light where the PMT is not sensitive. It is solar-blind, whereas the Si-diode also has quantum efficiency for visible light. So the filters limit the spectrum to small regions in the VUV range. Moreover they are used to select an area of the lamp's spectrum where it is continuous. The transmission curves of these vacuum monochrometers are shown in Figure 10 and in appendix #3. The filters have a diameter of $1" = 2.54\ cm$ and further specifications are stated in Table 2.

Part No	Peak Wavelength	Maximal Transmission	FWHM
193-NB-1D	192.5 nm	21.4 %	25.0 nm
172-NB-1D	171.0 nm	17.5 nm	20.0 nm

Table 2: Specification of the used VUV filter based on the manufacturer's information [12]

To reduce scattered light and to control the solid angle, apertures of different sizes were fabricated. The white plastic ring is $14\ mm$ thick and its outer diameter is adapted to the vacuum tube's diameter ($\sim 40\ mm$). It is used to center the apertures by fixating them with three threaded rods and nuts which allows them to be easily changed.

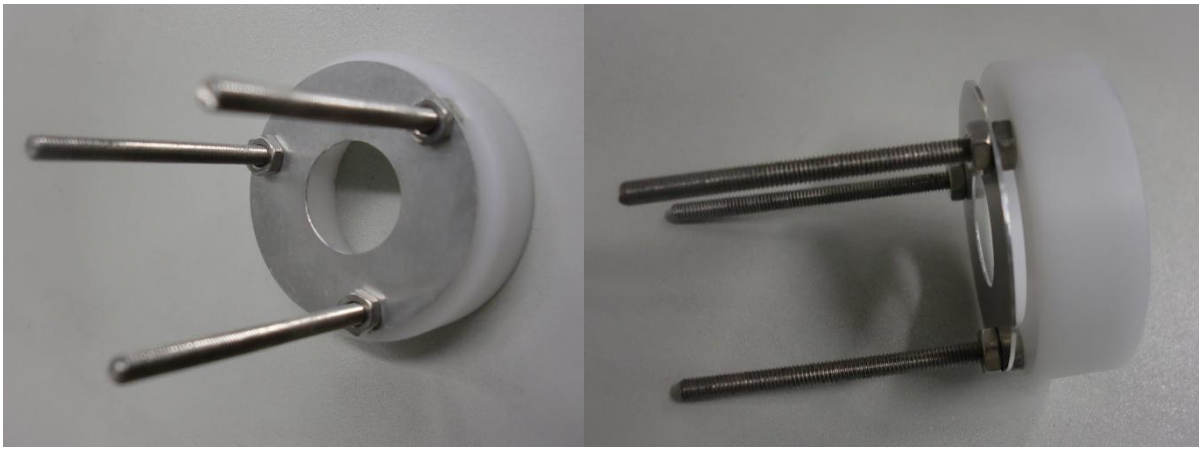

Figure 11: Pictures of an aperture for reducing scattered light and controlling the solid angles in the experiments

3.2.4 The Silicon Diode

Silicon diodes are standard instruments to detect photons via the photo effect. Normally they are only sensitive in the visible wavelength region but the diode used here was made for the detection in the VUV range.

The Si-detector was built by the company IRD (SXUV-100, serial number: 06-508) and has a size of $10\ mm$ x $10\ mm$. It was calibrated by the manufacturer in the wavelength range from $200\ nm$ to $1100\ nm$. Later on the National Institute of Standards and Technology (NIST, USA) has calibrated it from $52\ nm$ to $254\ nm$. This diode has already been used in an experiment before [13] where the fact that the detector's rim has a too high efficiency compared to the area in the middle, attracted attention. Therefore an aperture with a fixed diameter of $8\ mm$ was placed on the detector in order to shadow the rim. The application of the aperture has no influence on the calibration because the gauging for the middle area is still valid and only the rim has different quantum efficiency. Figure 12 shows on the left hand side the diode's quantum efficiency in the area of $50\ nm$ to $1100\ nm$ and on the right hand side the area where the optical filter with the peak transmission at $192.5\ nm$ applies. There the average quantum efficiency is 6.36%. The data measured by NIST is listed in Table 7 in appendix #1.

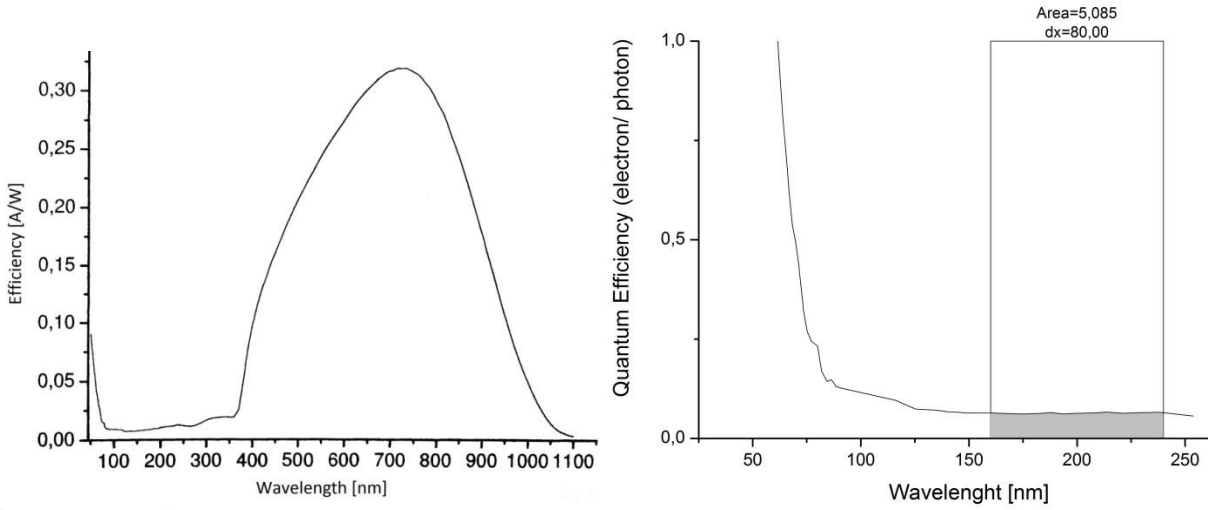

Figure 12: left: Efficiency of the Si-diode calibrated by NIST and IRD. [13] The diode has its largest efficiency in the area of visible light and a nearly constant efficiency in the VUV
right: Quantum efficiency of the diode in the VUV range. Average quantum efficiency in the filter 1 region ($\lambda_{peak} = 192.5\ nm$): $QE_1 = 6.36\%$; calibrated by NIST (compare Table 7)

3.2.5 The photomultiplier tube

To measure the low photon flux of the single photon source a PMT is used. A schematic cross-section is shown in Figure 13.

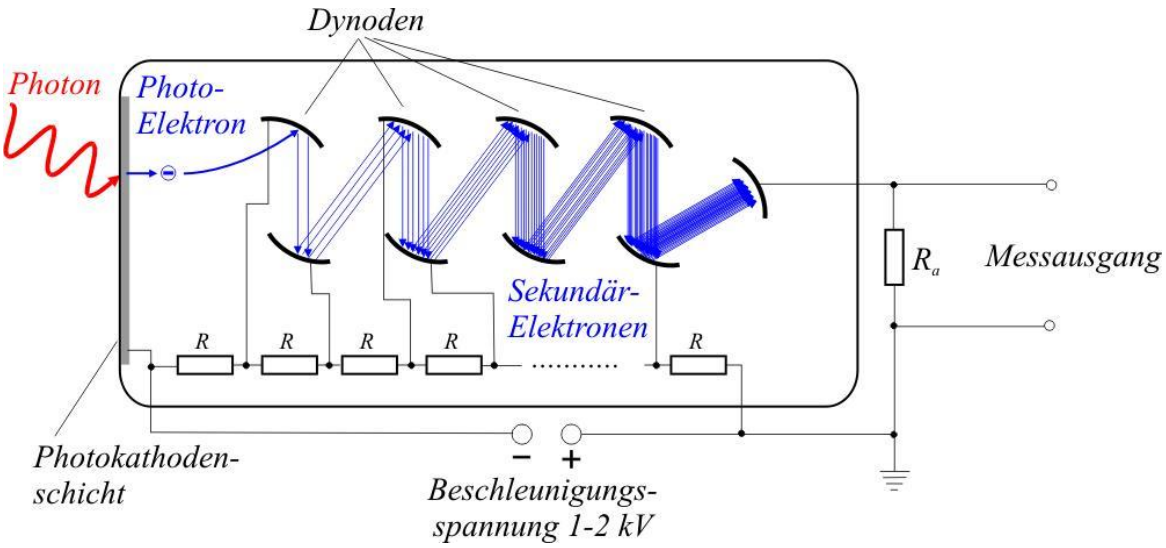

Figure 13: Schematic cross-section of a head-on PMT with incoming photons on the left and measuring output on the right [14]

If a photon hits the photocathode it may create a primary electron via the photo effect. After that the electron is accelerated towards the first dynode that has a positive electrical potential compared to the cathode. By the process of secondary emission, the electron multiplies. As the next dynode's voltage is even higher, the electrons are accelerated towards it and then multiplied again. This process happens at every dynode which results in an exponential gain, depending on the applied voltage and the number of dynodes. Figure 14 shows on the right hand side the typical relation between the applied voltage and the gain.

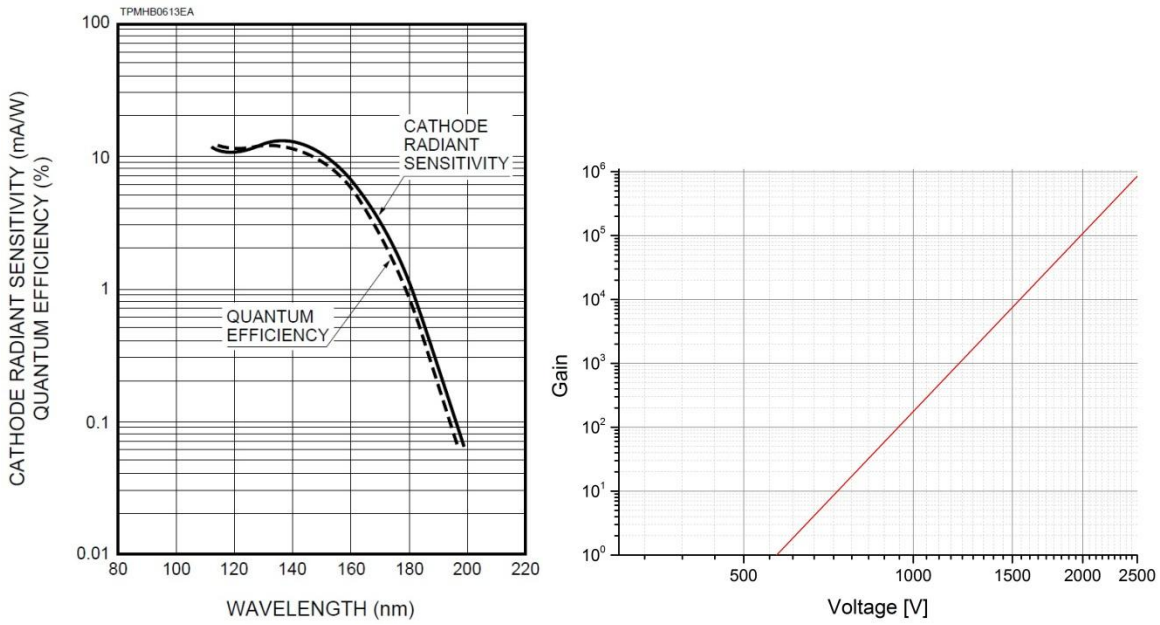

Figure 14: left: Quantum efficiency of the solar-blind PMT R6835
right: Voltage-depending gain for this PMT. Both curves are given by the manufacturer [15]

The PMT used in this experiment is the R1459 built by HAMAMATSU. The data sheet of this PMT was not available and could not be retrieved from HAMAMATSU. However, according to the manufacturer it has the same characteristics relating to quantum efficiency and gain like the R6835 which is the replacement product of the R1459. Both PMTs have a CsI photocathode, where the wavelength of maximal response is 140 nm, whereas the overall spectral response is $115\ nm$ to $200\ nm$. The maximal supply voltage is $2500\ V$ and the maximum average anode current is $0.1\ mA$ [16]. Figure 14 on the left hand side shows the quantum efficiency of the photomultiplier based on the manufacture's information.

The dark count rate (noise) of the PMT is < 1 Hz and therefore it can be neglected in the following.

4. Measurements with the PMT

4.1 Amplification Gain

After the alignment of the beam path, the PMT's gain was measured. Therefore the configuration showed in the beginning was used (see Figure 5) with the distance $d = 1205\ mm$ between the PMT's aperture and the lamp. The aperture was set to a diameter of $1\ mm$. The measurement was performed in vacuum for different filter configurations. The results are shown in the following Figure 15. Furthermore the gain given by the manufacturer is sketched in the diagram (blue line).

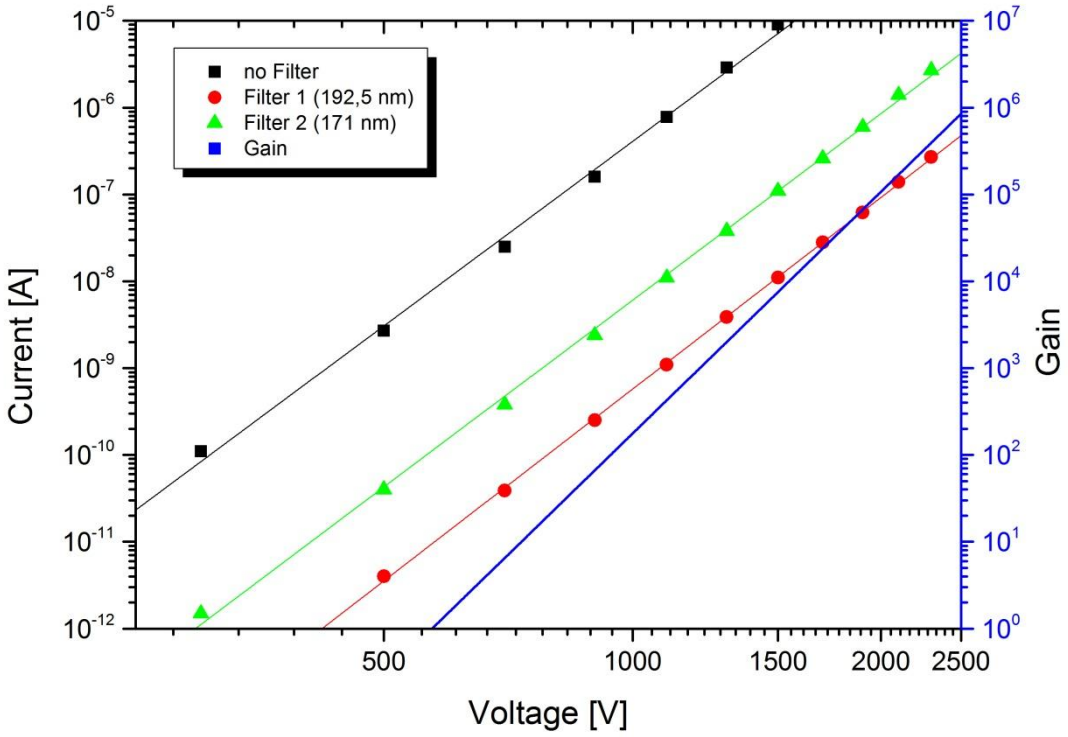

Figure 15: Typical current – voltage fit for the PMT. Here with a 1 mm aperture and a distance of 1205 mm to the lamp The manufacturer's gain is plotted as well (blue).

The different quantum efficiencies for light in the range of $171\ nm$ and light in the range of $192.5\ nm$ reflect the different offsets of the fits for the green and the red curve.

The measured data was linearly fitted with the function $y = ax + b$ and the average slope parameter of the three current lines was calculated to $a_1 = 7.17 \pm 0{,}10$. Whereas the linear fit of the manufacturer's gain has a slope parameter of $a_2 = 9{,}25 \pm 0{,}08$. The fit parameters vary by 29 %. Which is probably because of the PMT used here and the R6835 not having the same gain. During the measurement the intensity of the deuterium lamp which was controlled by the Si-diode, decreased about 1% which is much less than the difference between the two slopes. Without the

knowledge of the quantum efficiency the gain cannot be determined, because it is not known at witch voltage the gain is 1.

4.2 Homogeneity

The homogeneity of the PMT's active area was tested with respect to two degrees of freedom. First, the active area was illuminated by using different apertures from $1\ mm$ to $15\ mm$ diameter with a fixed distance to the lamp. This measurement was made twice with similar results. One is sketched in Figure 16. The distance between the D_2-Lamp and the apertures was $d = 545\ mm$. The measurement data can be seen in Table 9 in appendix #1.

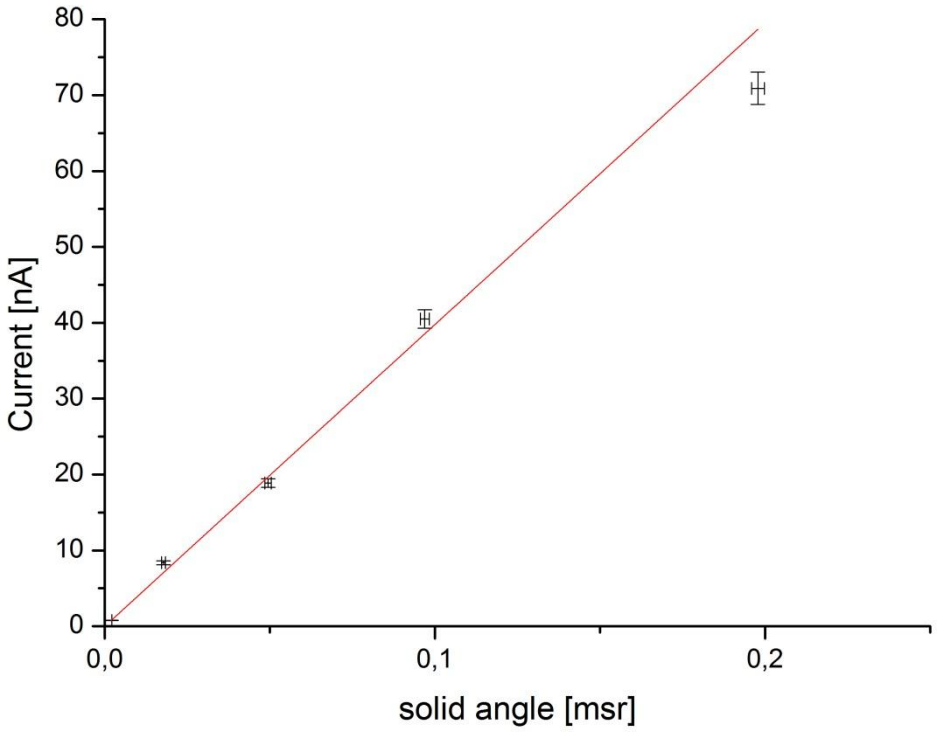

Figure 16: Measured PMT currents for different solid angles. The solid angles were realized by different aperture diameters with a fixed distance of $d = 545\ mm$ to the lamp.

The red curve is a linear fit. This means that the efficiency of the photo cathode is almost homogeneous as solid angle and current are direct proportional.

Second, the rotational symmetry of the PMT has been checked by turning the PMT several times in 60° steps. The configuration was the same as in the previous measurement but with a fix aperture with a diameter of $7mm$. The result is shown in Figure 17.

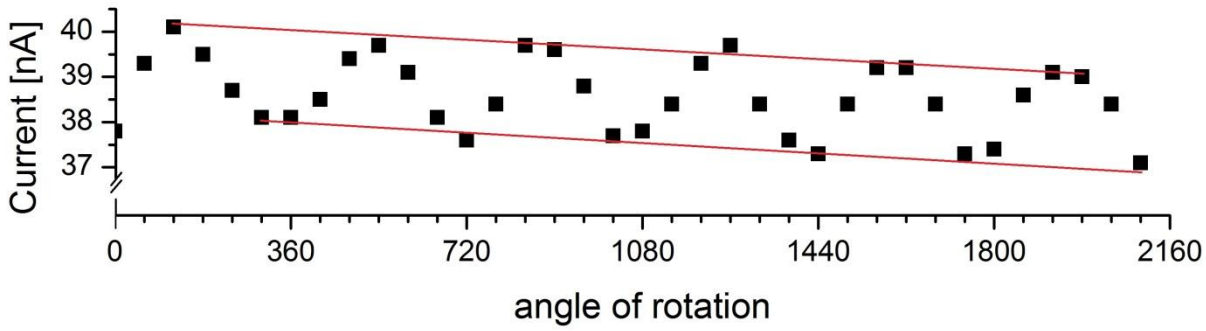

Figure 17: Relation between the PMT's angle of rotation and its current

Furthermore the measurement was made with other apertures and even without one to prove that this effect is independent of the illuminated area. The results were similar and show that the current is dependent on the position of the PMT. The difference between a maximum and a minimum is $\pm 3.3\%$ and the maxima/ minima are repeated every 360°. The decrease of the current over the time comes from the fluctuation of the lamp's intensity. Possible reasons for the different current could be the earth's magnetic field distracting the electrons in the PMT.

4.3 Calibration with the Silicon Diode

In order to be able to compare the current at the Si-diode with the PMT's current, it is necessary to check if the measured photo current scales with the difference of the solid angles.

Therefore the Si-diode was attached on the right side as in Figure 7 and afterwards on the left side. Because the mirror is not exactly in the middle of the cylinder the optical path on the right side is longer than the one on the left side. These path lengths were:

$$l_{right} = 370\ mm + 32\ mm + \sqrt{32^2 + 155^2}\ mm = 560\ mm \pm 9\ mm$$

$$l_{left} = 370\ mm + 155\ mm = 525\ mm \pm 7\ mm$$

This difference in the distance results in the following ratio of the solid angles.

$$\frac{\Omega_{left}}{\Omega_{right}} = \left(\frac{l_{right}}{l_{left}}\right)^2 = \left(\frac{560\ mm}{525\ mm}\right)^2 = 1.14 \pm 0.02$$

Furthermore the incident beam on the right side is not perpendicular. The active area decreases with increasing α, whereas α is the angle between the diode and the different reflection points at the mirror (Compare Figure 7).

$$\alpha = \sin^{-1}\frac{32\ mm}{155\ mm} = 12° \pm 7°$$

$\cos\alpha = 0.98 \pm 0.02$

All together there should be following geometrical difference in the intensities between the two sides:

$$\frac{I_{left}}{I_{right}} = 1.14 \cdot 1.02 = 1.16 \pm 0.03$$

In the experiment the measurements were made several times. One typical result can be seen in Table 3. The average ratio of photocurrents measured at the left and right side was $\frac{I_{left}}{I_{right}} = 1.14$ with a standard deviation of ± 0.01. Within the uncertainties experiment and geometrical consideration do match.

	Without filter	Filter 1 $\lambda_{peak} = 192.5nm$	Filter 2 $\lambda_{peak} = 171.0nm$
Si-diode on the right	39.6 nA	432 pA	408 pA
Si-diode on the left	45.6 nA	487 pA	464 pA

Table 3: Typical photo currents at the Silicon diode

4.3.1 PMT measurements in the 'current mode'

At first the PMT was operated in the 'current mode'. This means that the photon flux is big enough to measure a constant current at the last dynode. Here not only the quantum efficiency is unknown, but also the gain of the PMT does not match with the manufacturer information and thus it is also unknown. On the one hand this can be seen in the different slopes of the gain figures as shown above. On the other hand the measured current can be divided through the gain given by the manufacturer. The result should be a constant photo current before it gets amplified. This current is calculated in the following where N is the number of photons, QE is the quantum efficiency, and e the elementary charge. As the number of photons does not change over a short time and the other factors are constants, I_{Photo} has to be constant.

$$I_{Photo} = N_{ph} \cdot QE \cdot e$$

$$= \frac{I_{measurement}}{Gain_{manufacturer}} \stackrel{!}{=} const$$

To check if I_{Photo} is constant, a measurement was made with the distance $d = 1205\ mm$ between the lamp and the PMT's aperture with the diameter of $1\ mm$. This measurement was also made several times with similar results. The following Figure 15 shows one typical measured current and the photo current corrected for the gain given by the manufacturer.

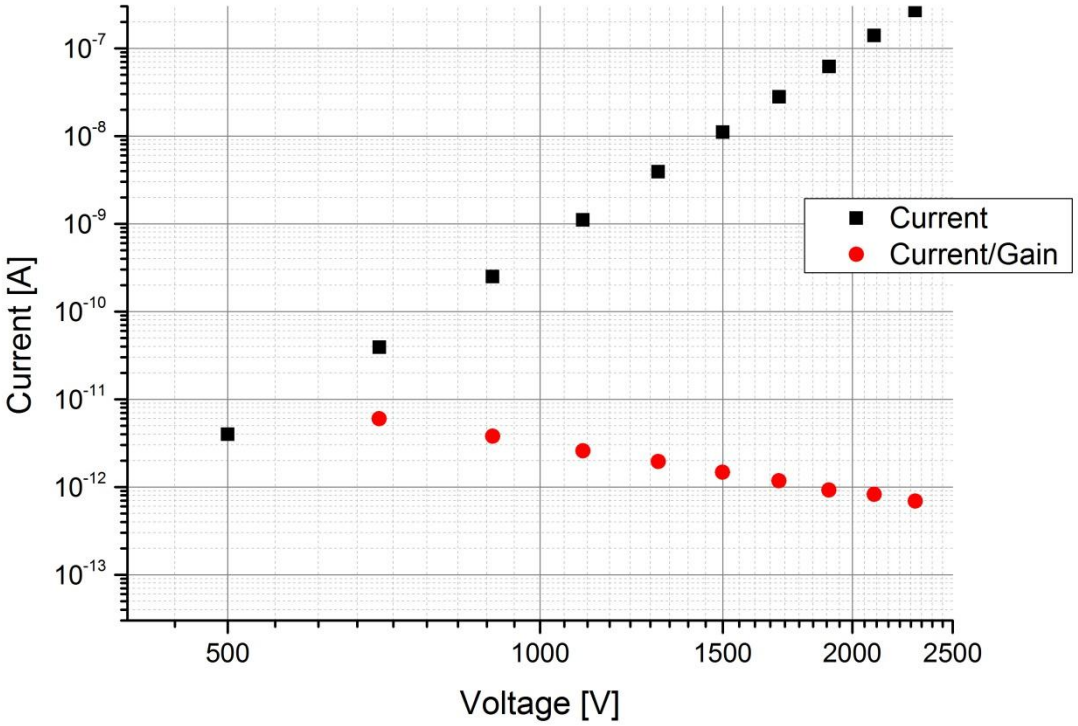

Figure 18: The PMT's current with respect to the applied voltage (black) and the current divided by the manufacturer's gain which can be seen in Figure 15 (red)

In this measurement the lamp's intensity decreased about 1%, whereas the initial photo current (red graph in Figure 18) would decrease about 90%. Therefore the function of the gain given by the producer is wrong and cannot be used for further calculations. So the calibration can only be done in the 'photon counting mode'.

4.3.2 Measurements in the 'photon counting mode'

In this mode the PMT is operated with the maximal voltage ($U_{max} = 2500\ V$) so the amplified signal of a single photon is measurable. These single photon signals are counted and therefore the size of the gain which only influences the signal height is not important.

Due to the comparison of the solid angle at the Si-diode and the one at the PMT's aperture and with the help of the Silicon diode's measured current ($I_{Si-Diode} = (416 \pm 8)\ pA$) and quantum efficiency, the photon flux at the PMT can be calculated.

$$\Omega_{Si-diode} = \frac{A}{d^2} = \frac{(4\ mm)^2 \cdot \pi}{(560\ mm)^2} = (1.60 \pm 0.10) \cdot 10^{-4}\ sr$$

$$\Omega_{PM} = \frac{A}{d^2} = \frac{(0.5\ mm)^2 \cdot \pi}{(370\ mm + 175\ mm + 660mm)^2} = (5.4 \pm 0.5) \cdot 10^{-7} sr$$

$$Rate_{PM,\ 192.5\ nm} = \frac{I_{Si-diode}}{e \cdot QE_{Si-diode}} \cdot \frac{\Omega_{PM}}{\Omega_{Si-diode}} = \frac{416\ pA}{e \cdot 6.36\%} \cdot \frac{5.41 \cdot 10^{-7} sr}{1.60 \cdot 10^{-4}\ sr} = (138 \pm 16)\ MHz$$

This value is compared to the measured rate of $(112 \pm 2)\ kHz$ in the next chapter.

4.4 Determination of the quantum efficiency

To calculate the quantum efficiency of the PMT it is necessary to know the number of photons, their spectral distribution, and the number of detected signals. As the spectrum of the D_2-lamp is continuous in the area where the filter with the peak wavelength of $192.5\ nm$ has transmittance (Figure 10), the spectral distribution depends only on the transmission curve of the filter. Also the Si-diode has almost constant quantum efficiency in the range from $160\ nm$ to $240\ nm$ (Figure 12 on the right).

The shape of the quantum efficiency graph is dependent on the material of the photocathode. Therefore the difference of the 'real' curve to the manufacturer's curve can only be a constant factor β that moves the graph y-direction in a logarithmic scale. In the following β is calculated.

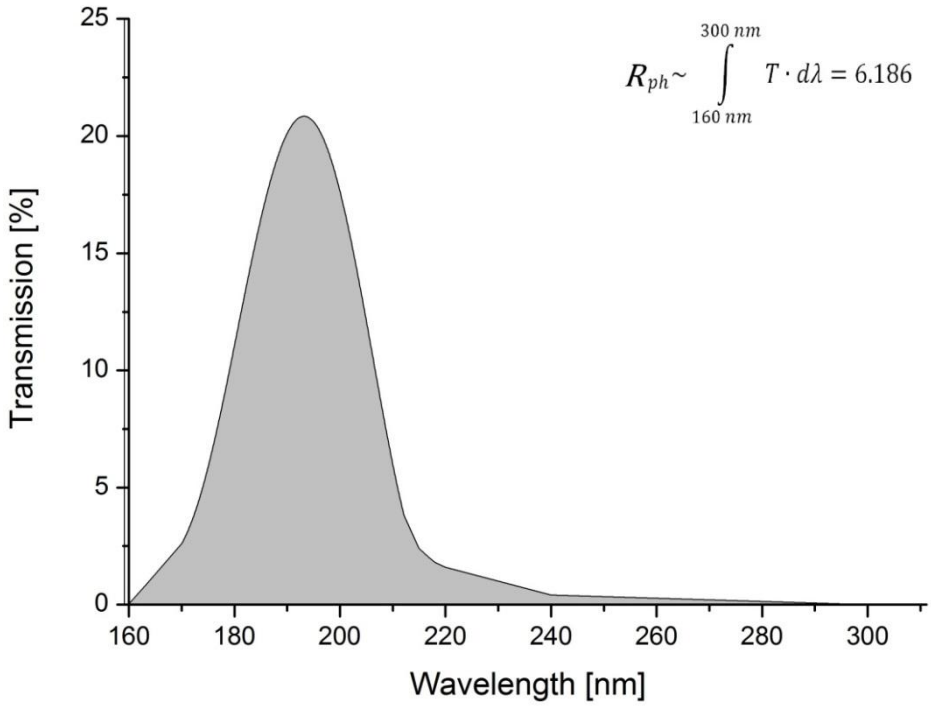

Figure 19: Area ($\sim Rate_{ph}$) underneath the optical filter curve with the peak wavelength of 192.5 nm

The following calculations are based upon the hypothesis that the quantum efficiency given by the manufacturer would be correct. As the rate and the spectrum of the photons are known, the area underneath the transmission line of the filter (Figure 19) is a measure for them. Areas $A(\lambda)$ with the width $d\lambda = 5\ nm$ underneath this line were multiplied with the corresponding producer's quantum efficiency.

$$R_{photons,\ detected} \sim \sum A(\lambda) \cdot QE(\lambda) = 0.03217$$

The sum over the whole wavelength range is 0.03217 and it's proportional to the rate of detected photons at the PMT. The quotient of this value to the whole area underneath the transmission line is equal to the quotient of the rate of detected to incoming photons. So the rate 'R' of detected photons can be calculated assuming that the manufacturer's information would be right:

$$\frac{0.03217}{6.186} = \frac{R_{photons,detected}}{138\ Mhz} => R_{photons,detected} = (718 \pm 83)\ kHz$$

Now this number is compared to the measured rate of detected photons and the ratio is used to correct the quantum efficiency given by the manufacturer.

$$\beta = \frac{718\ kHz}{112\ kHz} = 6.4 \pm 0.8$$

The factor 'β' was transferred to the quantum efficiency graph what can be seen in the following Figure 20.

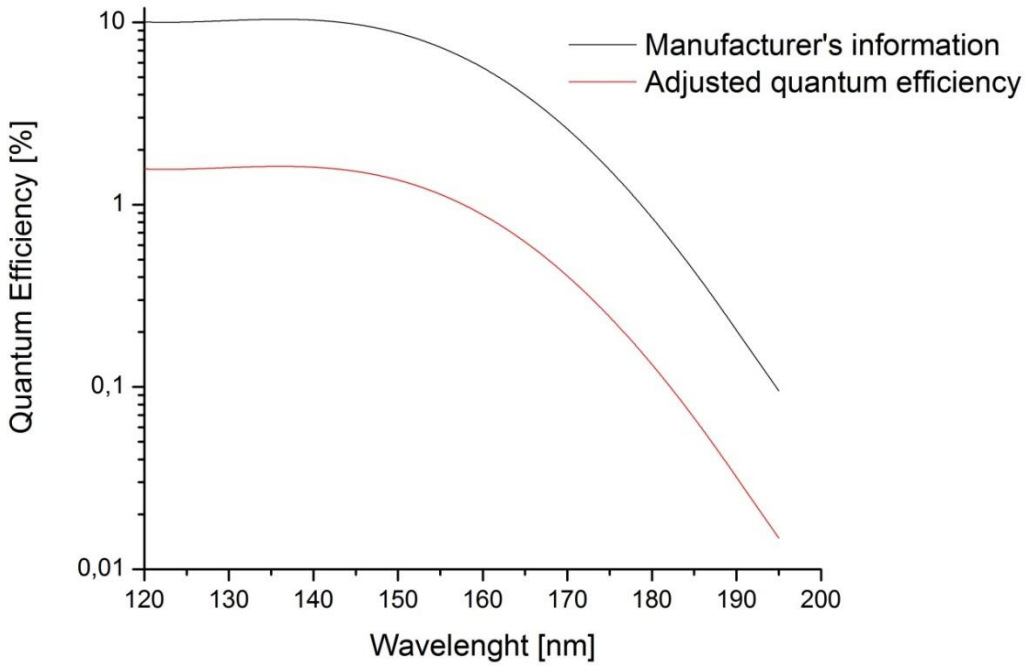

Figure 20: Manufacturer's and adjusted quantum efficiency. Numerical values are listed in appendix #1 Table 10

The measured quantum efficiency is smaller than the one given by the manufacturer. That is due to the age of the used photo cathode. It is more than 15 years old and therefore it may have aged which leads to a smaller quantum efficiency.

5. Intensity Calibration of the Xenon Photon Source

The Xenon photon source could now be calibrated with the help of the PMT. Therefore the PMT was attached to the photon source (see Figure 21) and the light yield was measured.

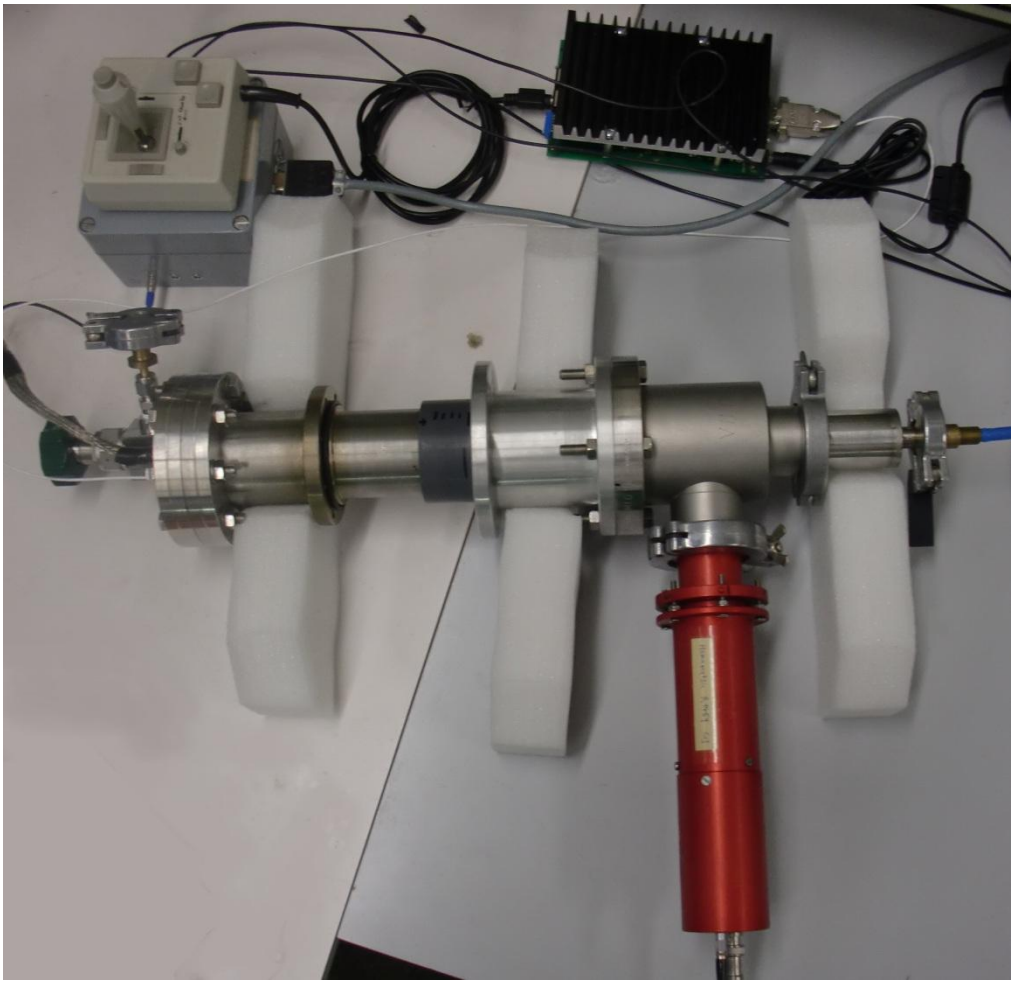

Figure 21: Picture of the Xenon photon source with the attached PMT (red) and the control of the PIN diode's motor (top left corner)

The intensity of the Xenon photon source was checked with two different methods. First the number of photons was controlled by the distance between the alpha source and the movable detector. Second the distance between the alpha source and the PIN diode was kept fixed. A $4 \text{ x} 10\ mm$ wide slit was set $1\ cm$ in front of the photon source's glass cylinder. This slit was moved in order to measure the intensity with respect to the observed area. Figure 22 shows a schematic sketch of the measurements.

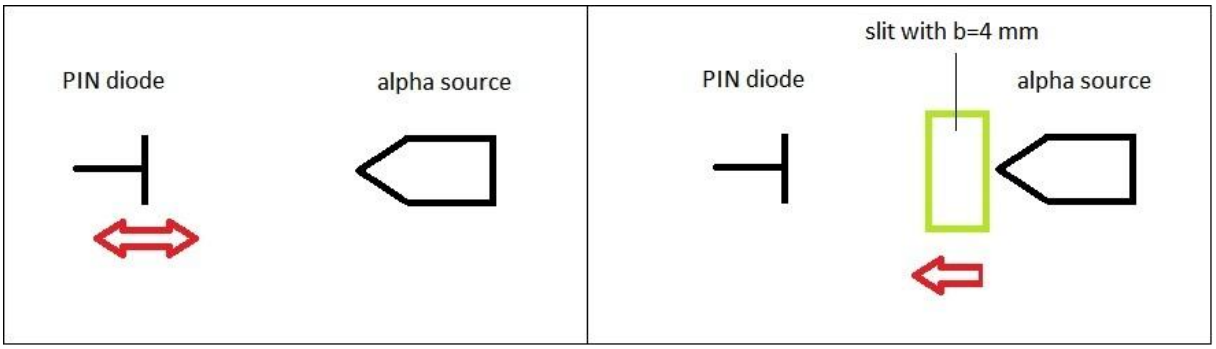

Figure 22: Schematic sketch of the two measurement methods
Left: The distance between alpha source and PIN diode was changed
Right: The distance between alpha source and PIN diode was fixed and a slit was moved from the alpha source to the PIN diode

In both measurements an aperture in front of the PMT was used to control the solid angle. The diameter was 15 mm for the first and 7 mm for the second measurement. The distance between the middle of the photon source's glass cylinder and the PMT's apertures was 57 mm. The setup is shown in Figure 23.

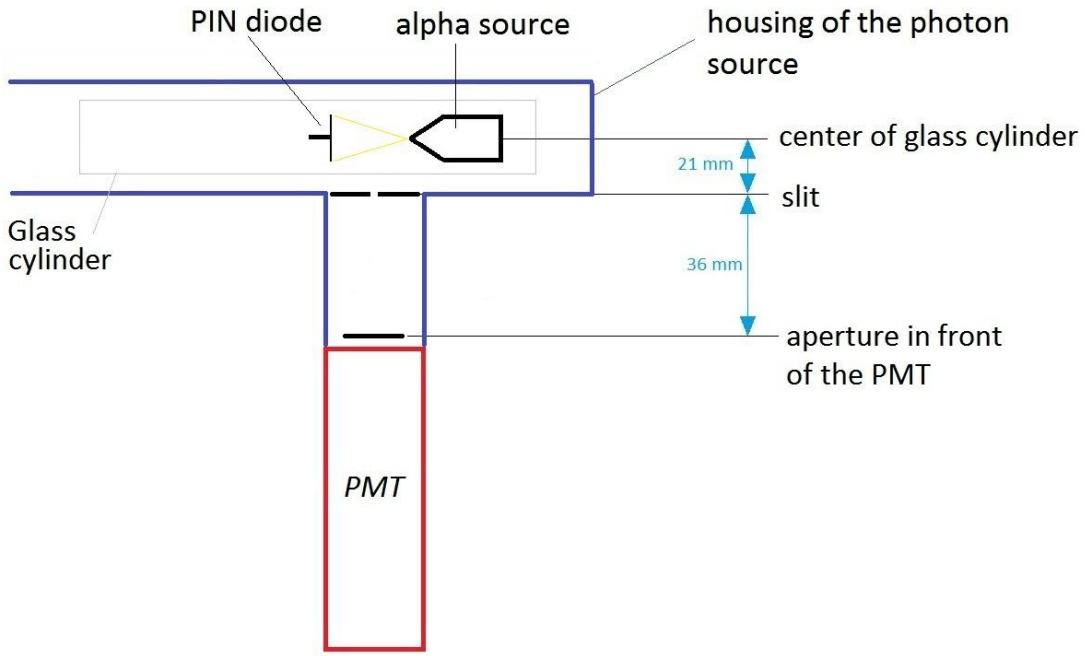

Figure 23: Schematic setup to measure the intensity of the single photon source

After a first series of measurements the volume of the photon source was evacuated and refilled with fresh Xenon gas (purity 5.9). The initial gas was about two years old. During the measurements the number of photons, alpha particles, and coincident signals were counted.

5.1 Measurements

5.1.1 Variable distance between PIN diode and alpha source

In this measurement the distance Dbetween alpha source and PIN diode was changed and so the number of photons was controlled. The distance D is in approximation indirect proportional to the square root of detected alpha particles.

$$N_\alpha \sim \frac{A}{D^2} => D \sim \frac{1}{\sqrt{N_\alpha}}$$

The measurements had a different duration, based on the rate of events. Thereafter the results were converted to the duration of one hour so they are easier to compare.

The following table shows the results of the measurements. The table contains the number of photons, the number of alpha particles, the number of coincident signals (simultaneous detection of an alpha particle and a photon), the signal height of the alpha particles detected in the Si-diode (~residual energy), and the ratio of coincident signals over number of alpha particles. The distance of the aperture (diameter 15 mm) to the center of the photon source's cylinder was 57 mm.

$$\Omega_{PMT} = \frac{A}{d^2} = \frac{\left(\frac{15\ mm}{2}\right)^2 \cdot \pi}{(57\ mm)^2} = (54 \pm 5)\ msr$$

$N_{single\ photons}$	N_α	Coincident signals	Energy [V]	$\frac{\text{Coincident signals}}{N_\alpha}$
6339	5313305	2316	5,2	$4{,}35 \cdot 10^{-4}$
9281	4467771	3346	4,5	$7{,}49 \cdot 10^{-4}$
12700	2974058	3362	4,2	$11{,}3 \cdot 10^{-4}$
15976	2049842	3212	3,8	$15{,}7 \cdot 10^{-4}$
22853	1008210	2796	3,0	$27{,}7 \cdot 10^{-4}$
29820	497852	2266	1,4	$45{,}5 \cdot 10^{-4}$

Table 4: Light Yield of the VUV photon source for various distances between Si-detector and alpha source with the two year old Xenon gas and a 15 mm aperture in front of the PMT. Measurement duration $t = 1\ h$.

It can be seen that the number of detected alpha particles decreases due to the decreasing solid angle. The number of uncorrelated photons rises, because fewer alpha particles were absorbed by the PIN diode due to its decreasing solid angle. This means more (undetected) alphas can deposit their full energy in the gas. Furthermore the detected alpha particles lose more of their energy in the gas and less energy in the PIN diode, which also leads to a greater number of photons. The number of coincident signals depends both on the rate of photons and alpha particles. Therefore the number of coincident photons first rises and then decreases. Another important quantity is the ratio between the coincident PMT signals and the number of detected alpha particles. This number rises constantly with increasing distance $d \sim 1/\sqrt{N_\alpha}$ what can be seen in Figure 24.

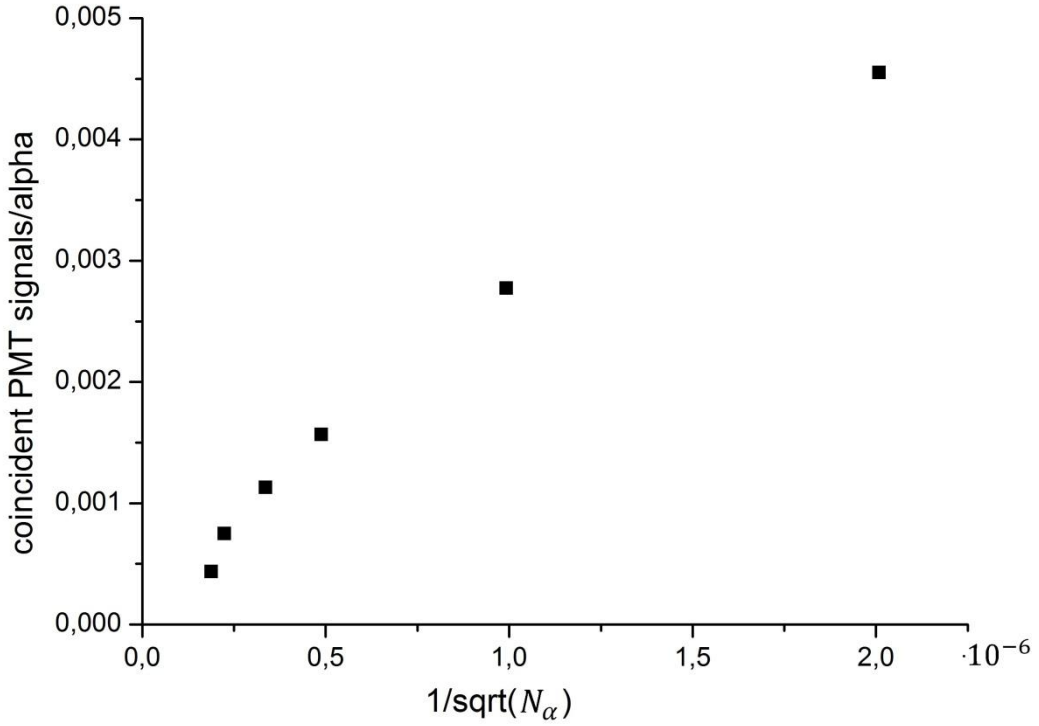

Figure 24: Light yield of the VUV photon source for various distances between Si-detector and alpha source. The data was taken with the two year old Xenon gas and a 15 mm aperture in front of the PMT. Measurement duration $t = 1\ h$.

The following measurements were done with the new Xenon gas at a pressure of $P = 1.2\ bar$. The set up did not change.

$N_{single\ photons}$	N_α	Coincident signals	Energy [V]	$\frac{\text{Coincident signals}}{N_\alpha}$
606660	4799754	212400	5,2	0,0443
1356000	3636270	452400	4,5	0,124
2688000	1591482	561000	3,5	0,353
3408000	755070	438000	2,6	0,580
3702000	398622	283800	1,5	0,712

Table 5: Light Yield of the VUV photon source for various distances between Si-detector and alpha source with two hours old Xenon gas and a 15 mm aperture in front of the PMT. Measurement duration $t = 1\ h$.

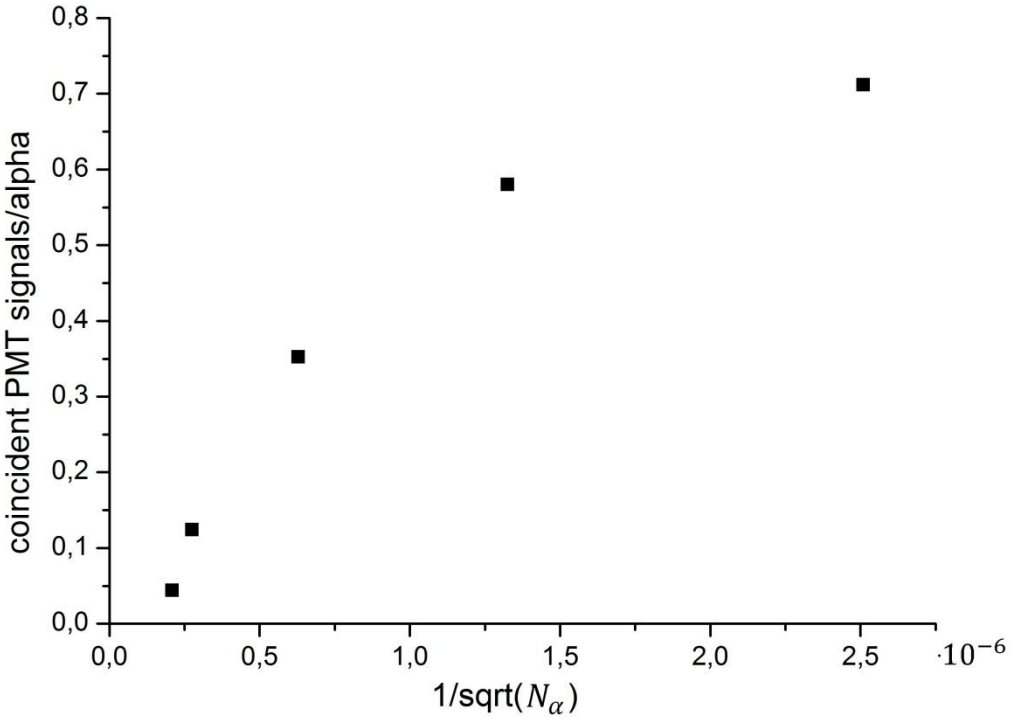

Figure 25: Light yield of the VUV photon source for various distances between Si-detector and alpha source. The data was taken with renewed Xenon gas and a 15 mm aperture in front of the PMT. Measurement duration $t = 1\ h$.

The number of coincident PMT signals per alpha particle increases about two orders of magnitude with the renewed gas. As the set-up can only count one coincident photon per alpha particle the rate cannot exceed 1. This saturation effect is clearly visible for large distances (see Figure 25).

5.1.2 Fixed distance between alpha source and PIN diode

In this measurement a slit was moved in front of the glass cylinder of the photon source as sketched in Figure 22 on the right. The slit was moved in 2.5 mm steps. In the first position it was partly shadowed by the alpha source. In the last two positions it got shadowed by the PIN diode. As the slit is 4 mm wide, the observed area is according to theorem of intersecting lines 6 mm wide. If the slit is moved 5 mm the total observed area is 11 mm wide. The distance between the PIN diode and the alpha source was about 1.5 cm. The results are listed in Table 6.

Position	photons	α	Correlated signals
1	2198	546457	104
2	3758	546560	278
3	2466	544992	254
4	1953	548561	299
5	921	546743	108
6	788	547689	9

Table 6: Light yield of the VUV photon source based on the position of the aperture relatively to Si-detector and alpha source

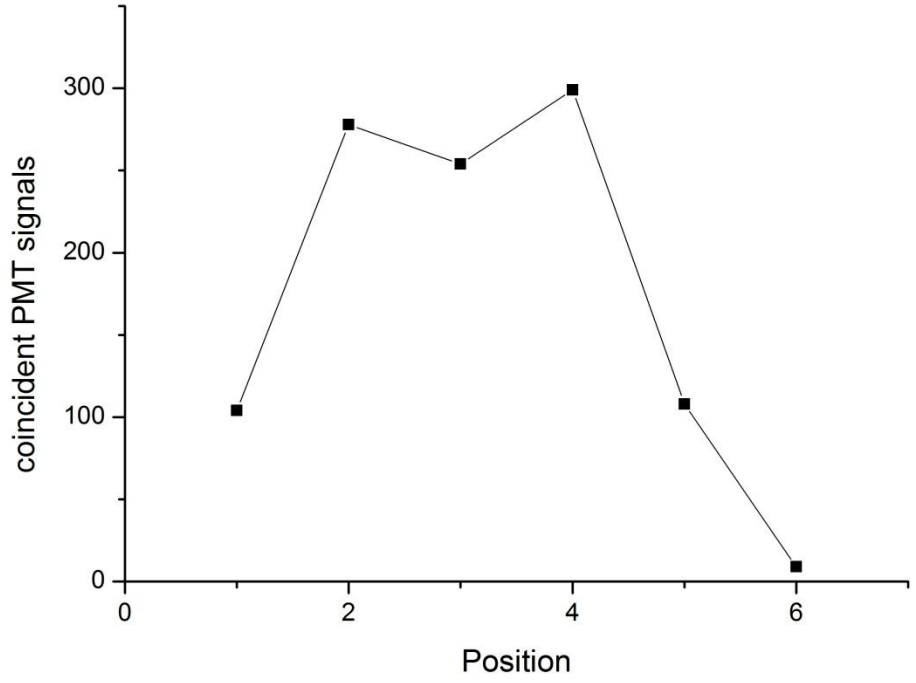

Figure 26: Light yield of the VUV photon source based on the position of the aperture relatively to Si-detector and alpha source

Figure 26 shows that the rate of photons is almost constant in a range larger than 11 mm before the slit gets (partly) shadowed by the PIN diode or the alpha source respectively.

5.2 Results and discussion

Table 5 shows that for the new gas a maximum of 0.712 photons were detected per alpha particle. The photons emitted by the Xenon molecules peak around at 174 nm. Weighting the emission spectrum with the PMT's quantum efficiency, results in an efficiency of $(0.29 \pm 0.04)\%$ for the analyzed wavelength spectrum.

Regarding the quantum efficiency there were 246 photons passing the aperture. The solid angle is $54\ msr$. Combining these to results the total number of emitted photons per α can be determinated:

$$\frac{N_{photons}}{\alpha} = \frac{246 \cdot 4\pi}{54\ msr} = (5.7 \pm 0.9) \cdot 10^4$$

This is about 48 % of the expected yield of $N_{ph} = 1.2 \cdot 10^5$photons per alpha particle. Possible reasons for the reduction are:

- The used setting cannot differentiate between a PMT signal of one incoming photon and the one of several incoming photons. This means that every time two photons at the PMT were detected at once the signal is treated like a single photon. This can be seen in the saturation in Figure 25.
- As the trigger signal of the alpha source should be used for the readout electronics, the alpha particles have to deposit some energy in the Si-detector. This means that the alpha particles cannot lose all their energy in the Xenon gas and therefore the number of $1.2 \cdot 10^5$ photons per alpha is too high. Here the particles had a residual energy of about 25 % of its initial energy.
- The Xenon gas was 90 minutes in the photon source until the measurement with the biggest distance between alpha source and Si-detector and so the largest rate of coincident signals per alpha particle was made. This time is enough to get an impurity and therefore to reduce the number of photons per alpha particle.

The influence of the age of the Xenon gas on the number of coincident signals per alpha is sketched in Figure 27. The measuring points have a similar residual energy at the Si-detector.

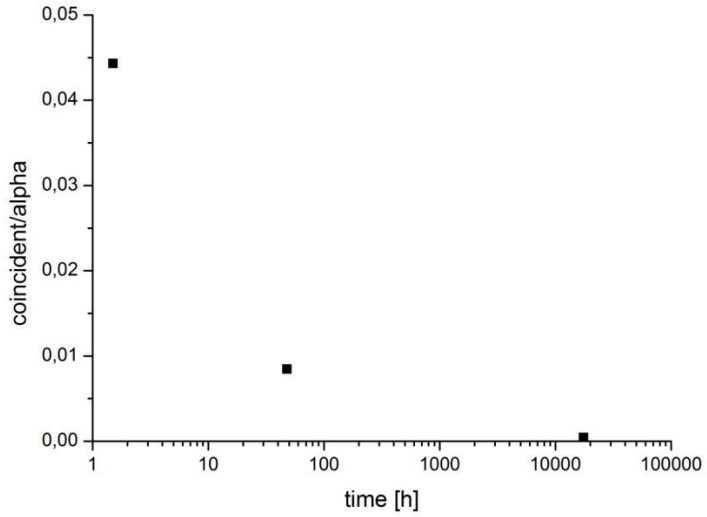

Figure 27: Ageing effect of the Xenon gas

It can be seen, that the age and thus the impurity of the Xenon gas has a great influence on the obtained photon yield. Especially in the very first hours the decrease of the photon rate is very high.

6. Summary and Outlook

In this thesis a calibration procedure for a new single photon source in the VUV wavelength region 160 – 200 nm was tested. The calibration was performed with the help of a photomultiplier tube and a Si-diode. The diode was calibrated to a primary standard by NIST, the National Institute of Standards and Technology in the USA.

Several measurements were made to transfer the calibration from the diode to the PMT and to check the different properties of the photomultiplier with a solar blind CsI photo cathode. At first it was proved that the sensitive cathode area is homogenous with respect to the radiated area. Secondly differences in the amplification were noticed, if the PMT's rotational degree of freedom was changed. All measurements were made with the same position of the detector, and results with different aperture diameters could be compared.

The determination of the PMT's quantum efficiency was performed with the help of the gauged Si-diode and a well-known amount of incoming photons, which was defined by the continuous spectrum of a deuterium arc lamp and the known transmission of two narrow band filters. The results of the present measurements differ from the manufacturer's information about the quantum efficiency by a factor of 6.4. The quantum efficiency of the PMT cathode integrated over the spectrum of the Xenon photon source is $QE_{PMT} = 0.29\ \%$.

With this result the light yield of the Xenon photon source was observed and normalized. The PMT was operated in the 'photon counting mode' and its signals were combined with the trigger signal of the PIN diode. With the obtained quantum efficiency the number of photons $N_{ph} = 5.7 \cdot 10^4$ per trigger signal was determined. This is about 48 % of the expectation for a purified Xenon gas. The losses are attributed to gas impurities stemming from outgassing surfaces.

In a next step the calibrated single photon source should be mounted at the RICH detector and the detector's response to single photons should be checked.

Appendix

#1 Tables

Wavelength [nm]	Quantum Efficiency (electron/ photon)		Wavelength [nm]	Quantum Efficiency (electron/ photon)
51,9	2,1601		125,4	0,0738
53,7	1,8442		135,4	0,0707
55,6	1,6199		140,3	0,0667
58,4	1,302		144,1	0,0659
62,2	0,9499		148,7	0,0634
63,9	0,8107		154,5	0,0637
65,7	0,6988		160,8	0,0635
66,9	0,616		164,8	0,063
68,3	0,5395		170	0,0618
69,9	0,4923		175	0,0615
71,2	0,4406		182,3	0,0626
73,5	0,3192		187,9	0,0648
75,2	0,2698		193,7	0,0616
77,1	0,2443		200	0,0632
80	0,2322		206,7	0,0638
81,8	0,1692		213,8	0,0658
84,4	0,1435		221,4	0,0631
86,5	0,1471		229,6	0,0651
88,6	0,1297		238,5	0,0654
92	0,1254		253,7	0,0558
116,4	0,095		121,6	0,0821
118	0,0912		125,4	0,0738
121,6	0,0821		135,4	0,0707

Table 7: Quantum efficiency of the Silicon Diode for the VUV by NIST [17]

Voltage [V]	no Filter	Filter 1 (192,5 nm)	Filter 2 (171 nm)	Gain
300	1,10E-10	0	1,50E-12	
500	2,70E-09	4,00E-12	4,00E-11	
700	2,50E-08	3,90E-11	3,80E-10	6,5
900	1,60E-07	2,50E-10	2,40E-09	66,4
1100	7,80E-07	1,10E-09	1,10E-08	4,28E+02
1300	2,90E-06	3,90E-09	3,80E-08	2,00E+03
1500	9,00E-06	1,10E-08	1,10E-07	7,51E+03
1700		2,80E-08	2,60E-07	23934
1900		6,20E-08	6,00E-07	67234
2100		1,40E-07	1,40E-06	1,69E+05
2300		2,70E-07	2,70E-06	3,92E+05

Table 8: Measurement of the PMT's current for different voltages. $d_{aperture} = 1\ mm\ L = 1205\ mm$

aperture diameter [mm]	Current [nA]	Ω [msr]	$\delta\Omega$ [msr]
1	0,77	0,0020	0,0002
3	8,38	0,0178	0,0006
5	18,87	0,0495	0,0010
7	40,5	0,0969	0,0014
10	70,9	0,1978	0,0020
15	135	0,445	0,003

Table 9: Current of the PMT for $L = 545\ mm$ and different apertures

Wavelength [nm]	Quantum Efficiency Manufacturer [%]	Quantum Efficiency Experiment [%]
120	10,04	1,57
125	10,03	1,57
130	10,22	1,60
135	10,37	1,62
140	10,27	1,60
145	9,74	1,52
150	8,71	1,36
155	7,28	1,14
160	5,63	0,88
165	3,98	0,62
170	2,59	0,40
175	1,55	0,24
180	0,85	0,13
185	0,43	0,07
190	0,20	0,03
195	0,10	0,02

Table 10: Quantum efficiency of the PMT

#2 The current meters

- **Pictures**

Figure 28: Photos of the amperemeters (left: model 614, right: model 602)

- Specifications

CURRENT

RANGE	RESOLUTION	ACCURACY (1 YR.) 18°-28°C ±(%rdg + digits)	TEMPERATURE COEFFICIENT 0°-18°C & 28°-35°C ±(%rdg + digits)/°C	MAXIMUM SUPPRESSION
20pA	10fA	1.5% + 5d*	0.1 % + 1 d	± 20pA
200pA	100fA	1.5% + 3d	0.1 % + 0.3d	±200pA
2000pA	1pA	1.5% + 1d	0.1 % + 0.3d	±200pA
20nA	10pA	0.5% + 2d	0.02% + 0.3d	± 20nA
200nA	100pA	0.5% + 1d	0.02% + 0.3d	±200nA
2000nA	1nA	0.5% + 1d	0.02% + 0.3d	±200nA
20μA	10nA	0.3% + 2d	0.01% + 0.3d	± 20μA
200μA	100nA	0.3% + 1d	0.01% + 0.3d	±200μA
2000μA	1μA	0.3% + 1d	0.01% + 0.3d	±200μA

*With current suppress.

INPUT BIAS CURRENT: Less than 60fA at 23°C.
INPUT VOLTAGE BURDEN: Less than 200μV.
PREAMP SETTLING TIME (to 1% of final value): pA, 0.6s. nA, 5ms. μA, 2.5ms.
NMRR: pA and nA, 70dB. μA, 55dB. At 50Hz and 60Hz.
MAXIMUM OVERLOAD: pA and nA, 350V peak. μA, 75V peak.

AS A VOLTMETER:
RANGE: .001V full scale to 10V in nine 1X and 3X ranges.
ACCURACY: ±1% of full scale on all ranges exclusive of noise and drift.
ZERO DRIFT: Less than 1mV per 24 hours, less than 150μV per °C.
METER NOISE: ±25μV maximum with input shorted on most sensitive range.
INPUT IMPEDANCE: Greater than $10^{14}\Omega$ shunted by 20pF. Input resistance may also be selected in decade steps from 10 to $10^{11}\Omega$.

AS AN AMMETER:
RANGE: 10^{-14}A full scale to 0.3A in twenty-eight 1X and 3X ranges.
ACCURACY: ±2% of full scale on 0.3 to 10^{-11}A ranges using the smallest available multiplier setting; ±4% of full scale on 3 × 10^{-12} to 10^{-14}A ranges.
METER NOISE: Less than ±3 × 10^{-15}A.
OFFSET CURRENT: Less than 5 × 10^{-15}A.

AS AN OHMMETER:
RANGE: 100Ω, full scale to $10^{13}\Omega$ in twenty-three linear 1X and 3X ranges.
ACCURACY: ±3% of full scale on 100 to $10^{9}\Omega$ ranges using the largest available multiplier setting; ±5% of full scale on 3 × 10^{9} to $10^{13}\Omega$ ranges.

AS AN COULOMBMETER:
RANGE: 10^{-13}C full scale to 10^{-6}C in fifteen 1X and 3X ranges.
ACCURACY: ±5% of full scale on all ranges. Drift due to offset current does not exceed 5 × 10^{-15}C per second.

AS AN AMPLIFIER:
INPUT IMPEDANCE: Greater than $10^{14}\Omega$ shunted by 20pF. Input resistance may also be selected in decade steps from 10 to $10^{11}\Omega$.
OUTPUTS: Unity-gain output and either voltage or current recorder output.
UNITY-GAIN OUTPUT: At DC, output is equal to input within 10 ppm, exclusive of noise and drift, for output currents of 100μA or less. Up to 1mA

Figure 29: Current specification of the KEITHLEY 614 (left) and the 602 (right) based on manufacturer's information

#3 The VUV filter

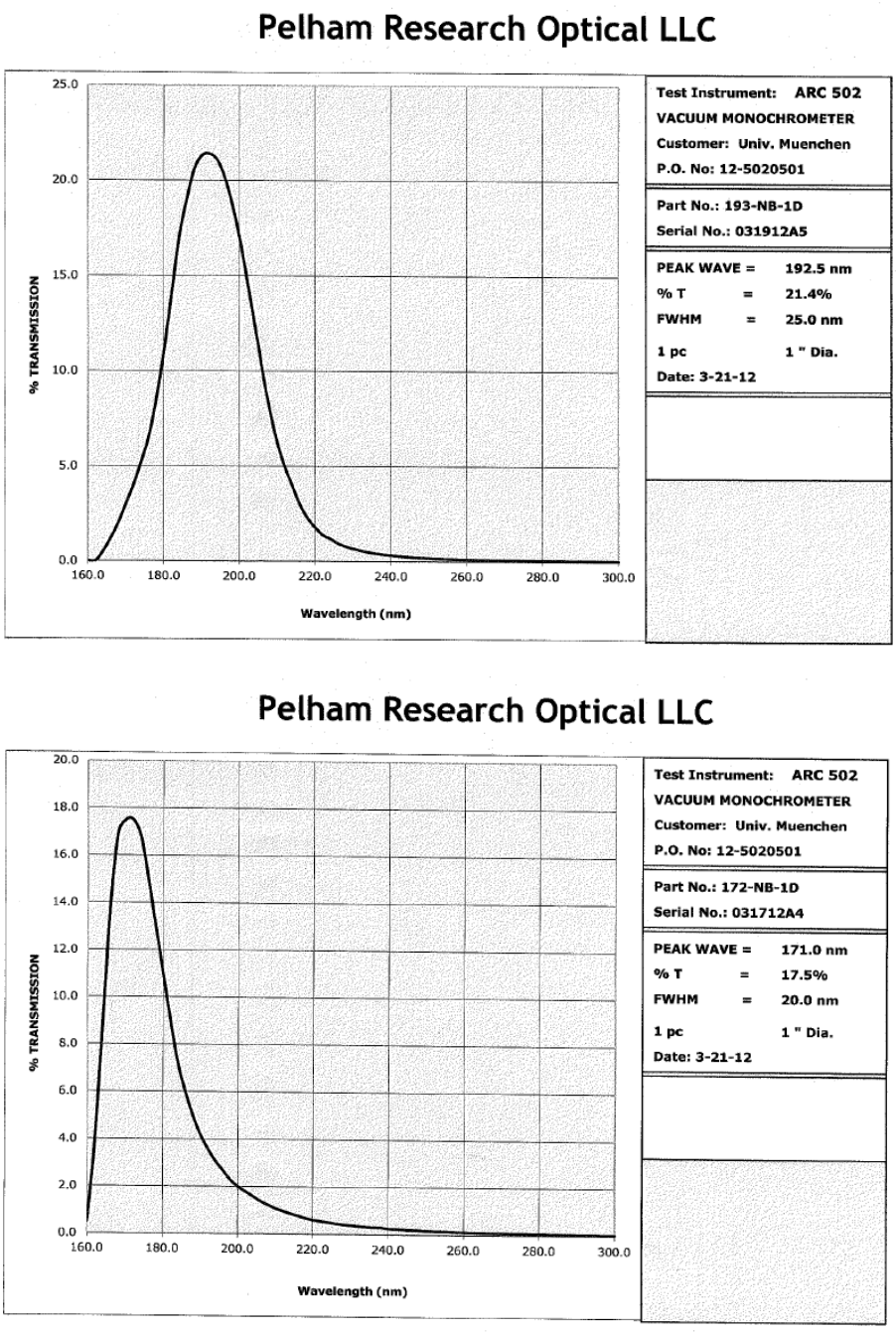

Figure 30:Transmisison curves given by the manufacturer[12]

Bibliography

[1] "The high-acceptance dielectron spectrometer HADES", G. Agakichiev et al., Eur. Phys. J., vol. A 41, pp. 243277 (2009).
[2] "The HADES RICH Detector", K. Zeitelhack et al., Nucl. Instr. Meth. A433, pp. 201 (1999)
[3] J. Friese and P. Huck, "Eine neue VUV Lampe zur Messung einzelner Photonen mit dem HADES RICH", *Verhandl. DPG(VI) 46, 2/92 (2011)*
[4] Absolute Number of Scintillation Photons Emitted by Alpha Particles in Rare Gases, K. Saito, H. Tawara, T. Sanami, E. Shibamura, and S. Sasaki
[5] Huck, P. Eine neue VUV Lampe yur Messung einzelner Photonen mit dem Hades RICH
[6] Heraeus Quarzglas GmbH Reinhard - Heraeus Ring 29; D-63801 Kleinsosthein
[7] A. Ulrich, private communication
[8] KEITHLEY – instruction manual of the 602 and 614
[9] *BCR Information Applied Meteorology - Deuterium lamps as Transfer standard*
[10] D.A. Skoog, J. L.. *Instrumentelle Analytik*
[11] T. Dandl, private communication
[12] Pelham Research Optical LLC. Manufacturer's information
[13] T. Heindl Diplomarbeit
[14] http://upload.wikimedia.org/wikipedia/commons/a/ab/Photomultiplier_schema_de.png
[15] Datasheet of the R6835 PMT by HAMAMATSU: http://sales.hamamatsu.com/assets/pdf/parts_R/R6835.pdf
[16] HAMAMATSU catalogue p. 38, 39: "Head-on Photomultiplier Tubes"
[17] United states department of commerce – National Institute of Standards and Technology – Report of Measurement, Ref:P.O.# 000256, Feb 8, 2007

Danksagung

Zunächst möchte ich Herrn Prof. W. Henning danken, dass er mir ermöglichte diese Arbeit zu schreiben.

Weiterhin gilt mein Dank meinem Betreuer Dr. J. Friese der mich immer wieder auf den rechten Weg zum Ziel geführt hat.

Auch bedanken will ich mich bei Dr. R. Gernhäuser, T. Dandl und dem Rest des E12 Teams die mir hilfreiche Ideen gegeben haben.

Ebenfalls gilt dem Werkstattteam mein Dank, die mir meine vielen Blenden konstruiert haben.

Zuletzt noch ein großes Dankeschön an meine Familie und Freunde, die mich immer und insbesondere in den letzten Wochen unterstützt haben.